Alternative schemes of predicting lepton mixing parameters from discrete flavor and *CP* symmetry

Jun-Nan Lu[*] and Gui-Jun Ding[†]

Interdisciplinary Center for Theoretical Study and Department of Modern Physics,
University of Science and Technology of China, Hefei, Anhui 230026, China
(Received 21 October 2016; published 17 January 2017)

We suggest two alternative schemes to predict lepton mixing angles as well as *CP* violating phases from a discrete flavor symmetry group combined with *CP* symmetry. In the first scenario, the flavor and *CP* symmetry is broken to the residual groups of the structure $Z_2 \times CP$ in the neutrino and charged lepton sectors. The resulting lepton mixing matrix depends on two free parameters θ_ν and θ_l. This type of breaking pattern is extended to the quark sector. In the second scenario, an Abelian subgroup of the flavor group is preserved by the charged lepton mass matrix and the neutrino mass matrix is invariant under a single remnant *CP* transformation, all lepton mixing parameters are determined in terms of three free parameters $\theta_{1,2,3}$. We derive the most general criterion to determine whether two distinct residual symmetries lead to the same mixing pattern if the redefinition of the free parameters $\theta_{\nu,l}$ and $\theta_{1,2,3}$ is taken into account. We have studied the lepton mixing patterns arising from the flavor group S_4 and *CP* symmetry which are subsequently broken to all of the possible residual symmetries discussed in this work.

I. INTRODUCTION

The neutrino oscillation experiments have made great progress in the last twenty years [1–3]. It has been firmly established that neutrinos must be massive particles and different flavor eigenstates are mixed. The three lepton mixing angles θ_{12}, θ_{13}, and θ_{23} as well as two mass squared differences Δm_{21}^2 and Δm_{31}^2 have been precisely measured [4–7]. However, we still do not know the neutrino mass ordering ($\Delta m_{31}^2 > 0$ or $\Delta m_{31}^2 < 0$), and the signal of *CP* violation in the lepton sector has not been observed. The preliminary T2K data favor a maximal Dirac *CP* violation phase $\delta_{CP} \simeq -\pi/2$ [8], and the latest global fits of neutrino mixing parameters show a weak evidence for a negative Dirac phase $-\pi < \delta_{CP} < 0$ [5–7]. The primary objectives of near future neutrino experiments are to determine the ordering of the neutrino masses and to measure the value of δ_{CP}.

On the theoretical side, the origin of neutrino mass and lepton flavor mixing is still unknown, although there have been lots of theoretical studies. Motivated by the observation that the simple tribimaximal mixing possibly originates from a A_4 flavor group, non-Abelian discrete flavor symmetry has been extensively exploited to explain the observed lepton mixing angles. Many other symmetries such as S_4, A_5, $\Delta(3n^2)$, $\Delta(6n^2)$, etc., have been considered over the years. Please see Refs. [9–13] for a review on discrete flavor symmetry and its application in model building. Significant progress in recent years is the precise measurement of the reactor mixing angle θ_{13} [14–18]. The

discovery of a somewhat large value of θ_{13} rules out the tribimaximal mixing patterns and many flavor models which predicted small or zero θ_{13}. Many approaches have been pursued to explain such a largish θ_{13}. Within the paradigm of the discrete flavor symmetry, a model-independent scan of the lepton sector reveals that only large flavor symmetry groups (e.g. $(Z_{18} \times Z_6) \rtimes S_3$ with the group identification [648, 259]) can produce mixing patterns compatible with experimental data and the Dirac *CP* phase is generally trivial if the whole lepton mixing matrix is fully fixed by the symmetry alone [19–23]. In this approach, the lepton flavor mixing matrix is determined by the assumed residual symmetries and their embedding into the parent flavor symmetry group, and the breaking mechanism is irrelevant; i.e., we do not need to consider how the vacuum configuration achieving the residual symmetries is dynamically realized.

In order to accommodate a nonzero θ_{13} and a nontrivial Dirac *CP* phase simultaneously, it is interesting to combine flavor symmetry with *CP* symmetry. This approach can generate a rich structure of mixing patterns which are in good agreement with the experimental data, and it allows us to predict all the mixing angles and *CP* phases in terms of a small number of input parameters [24–26]. From the bottom-up point of view, the generic neutrino and charged lepton mass matrices have both residual *CP* symmetry and residual flavor symmetry, and the residual flavor symmetry can be generated from the residual *CP* transformations [27–29]. Hence, it is natural to assume that the residual flavor and *CP* symmetry arises from a large flavor and *CP* symmetry group at the high energy scale. In this approach, the *CP* symmetry nontrivially acts on the flavor space such

[*]hitman@mail.ustc.edu.cn
[†]dinggj@ustc.edu.cn

that the consistency condition $X\rho^*(g)X^{-1} = \rho(g')$ has to be fulfilled in order for the theory to be consistent [24,30–32], where X is the CP transformation and $\rho(g)$ is the representation matrix of the element g contained in the flavor group. There has been intense theoretical activity on the flavor symmetry in combination with CP symmetry. Many flavor symmetry groups and their predictions for lepton mixing parameters have been studied such as A_4 [33–37], S_4 [24,38–43], A_5 [44–47], $\Delta(27)$ [48,49], $\Delta(48)$ [50,51], $\Delta(96)$ [52], and $\Sigma(36 \times 3)$ [53] as well as $\Delta(3n^2)$ [54,55], $\Delta(6n^2)$ [54,56,57], and $D_{9n,3n}^{(1)}$ [58] group series for a generic integer n. Recently, a comprehensive scan of leptonic mixing parameters which can be obtained from finite discrete groups of order less than 2000 and CP symmetry has been performed [59]. Moreover, the phenomenological implications of flavor and CP symmetry in neutrinoless double decay [37,39,43,44,57–60] and leptogenesis [59–61] have been investigated. It is remarkable that the residual CP symmetry provides a bridge between flavored leptogenesis and low energy leptonic CP violation.

It is usually assumed that the residual flavor symmetry in the charged lepton is an Abelian subgroup which can distinguish among the three generations, and the residual symmetry in the neutrino sector is a direct product of Z_2 and CP. As a consequence, the lepton mixing matrix turns out to depend on a single real parameter θ, and all mixing parameters are strongly correlated with each other. In the present work, we shall discuss the other possible approaches to predict lepton mixing parameters from flavor and CP symmetry, and two scenarios will be considered. In the first one, the neutrino and charged lepton mass matrices are invariant under two distinct $Z_2 \times CP$ subgroups. Consequently, all mixing parameters including mixing angles and CP phases are predicted in terms of two real parameters θ_l and θ_ν. In the second scheme, the original flavor symmetry is broken down to a residual Abelian subgroup with three or more elements in the charged lepton sector while a single residual CP transformation is preserved by the neutrino mass matrix, the Pontecorvo-Maki-Nakagawa-Sakata (PMNS) mixing matrix would depend on three real parameters $\theta_{1,2,3}$. For an example, we present a detailed analysis for the S_4 flavor symmetry group and CP symmetry. All possible independent combinations of remnant symmetries and the predictions for lepton mixing parameters are studied analytically and numerically.

The paper is organized as follows. In Sec. II, we study the symmetry breaking pattern in which a flavor symmetry combined with a CP symmetry is broken to $Z_2 \times CP$ in both the neutrino and charged lepton sectors. The resulting consequence for the prediction of the lepton mixing matrix is discussed, and the technical steps in the derivation are explained. We derive the conditions under which two distinct residual symmetries give rise to the same mixing pattern. Moreover, we analyze the independent mixing patterns which can be obtained from the popular flavor group S_4

and CP in this scheme. In Sec. III, our approach is extended to the quark sector. In Sec. IV, we explore another proposal in which the charged lepton and neutrino mass matrices are invariant under the action of a residual Abelian subgroup and a single CP transformation respectively. Finally, Sec. V concludes this paper. Moreover, Appendix A contains the necessary group theory of S_4 as well as its Abelian subgroups. Appendix B gives the conditions under which two distinct residual symmetries of the structure $Z_2 \times CP$ in both the up and down quark sectors lead to the same Cabbibo-Kobayashi-Maskawa (CKM) mixing matrix in the case that the fixed element is neither 0 nor 1.

II. LEPTON FLAVOR MIXING FROM RESIDUAL SYMMETRY $Z_2 \times CP$ IN BOTH CHARGED LEPTON AND NEUTRINO SECTORS

In the widely studied direct and semidirect approaches [11–13], it is assumed that the neutrino mass matrix m_ν possesses residual symmetry $Z_2 \times Z_2$ and $Z_2 \times CP$ respectively, and the charged lepton mass matrix is invariant under an Abelian subgroup contained in the flavor group. In this section, we shall be concerned with the scenario that the remnant symmetry preserved by both the neutrino and charged lepton mass matrices is of the structure $Z_2 \times CP$. Notice that the case of a flavor symmetry without CP broken to residual symmetries $G_e = Z_2$ in the charged lepton sector and $G_\nu = Z_2$ in the neutrino sector has been discussed in Refs. [62]. The three generations of left-handed leptons are assigned to a faithful irreducible triplet **3** of the flavor symmetry group.

A. General form of the PMNS matrix

We shall denote the residual Z_2 flavor symmetry of the charged lepton sector as $Z_2^{g_l} \equiv \{1, g_l\}$ with $g_l^2 = 1$, and the remnant CP transformation is X_l. In order for the theory to be consistent, the following consistency condition has to be fulfilled [24,39],

$$X_l\rho_{\mathbf{3}}^*(g_l)X_l^{-1} = \rho_{\mathbf{3}}(g_l^{-1}) = \rho_{\mathbf{3}}(g_l), \qquad (2.1)$$

where $\rho_{\mathbf{3}}(g_l)$ denote the representation matrix of the element g_l in the three-dimensional representation **3**. The charged lepton mass matrix $m_l^\dagger m_l$ is invariant under the action of the residual symmetry $Z_2^{g_l} \times X_l$, and it fulfills [24,39,42,43]

$$X_l^\dagger m_l^\dagger m_l X_l = (m_l^\dagger m_l)^*, \qquad (2.2a)$$

$$\rho_{\mathbf{3}}^\dagger(g_l)m_l^\dagger m_l \rho_{\mathbf{3}}(g_l) = m_l^\dagger m_l. \qquad (2.2b)$$

The unitary transformation U_l which diagonalizes the Hermitian matrix $m_l^\dagger m_l$ with $U_l^\dagger m_l^\dagger m_l U_l = \text{diag}(m_e^2, m_\mu^2, m_\tau^2)$ is strongly constrained by the postulated residual symmetry. In the following, we shall show how to determine U_l from $\rho_{\mathbf{3}}(g_l)$ and X_l. As the order of g_l is 2, the eigenvalues of $\rho_{\mathbf{3}}(g_l)$

are $(1, -1, -1)$ or $(-1, 1, 1)$, and we take the first case as an example without loss of generality. Assuming Σ_{l1} is a diagonalization matrix of $\rho(g_l)$ and it satisfies

$$\Sigma_{l1}^\dagger \rho_3(g_l) \Sigma_{l1} = \text{diag}(1, -1, -1) \equiv \hat\rho_3(g_l), \quad (2.3)$$

then we have

$$\rho_3(g_l) = \Sigma_{l1} \hat\rho_3(g_l) \Sigma_{l1}^\dagger. \quad (2.4)$$

The residual CP has to be consistent with the residual flavor symmetry, and therefore the following consistency condition should be fulfilled [43,58]:

$$X_l \rho_3^*(g_l) X_l^\dagger = \rho_3(g_l^{-1}). \quad (2.5)$$

Inserting Eq. (2.4) into the above equation and considering $g_l^2 = 1$, we get

$$X_l \Sigma_{l1}^* \hat\rho_3(g_l) \Sigma_{l1}^T X_l^\dagger = \Sigma_{l1} \hat\rho_3(g_l) \Sigma_{l1}^\dagger, \quad (2.6)$$

which leads to

$$(\Sigma_{l1}^\dagger X_l \Sigma_{l1}^*) \hat\rho_3(g_l) (\Sigma_{l1}^T X_l^\dagger \Sigma_{l1}) = \hat\rho_3(g_l), \quad (2.7)$$

which means

$$(\Sigma_{l1}^\dagger X_l \Sigma_{l1}^*) \hat\rho_3(g_l) = \hat\rho_3(g_l) (\Sigma_{l1}^\dagger X_l \Sigma_{l1}^*). \quad (2.8)$$

Therefore, $\Sigma_{l1}^\dagger X_l \Sigma_{l1}^*$ is a block diagonal and symmetric matrix, and its most general form is given by

$$\Sigma_{l1}^\dagger X_l \Sigma_{l1}^* = \begin{pmatrix} e^{i\xi_1} & 0 \\ 0 & u_{2\times 2}^l \end{pmatrix}, \quad (2.9)$$

where ξ_1 is an arbitrary real number and $u_{2\times 2}^l$ is a two-dimensional symmetric unitary matrix. We denote the Takagi factorization of $u_{2\times 2}^l$ as $\sigma_{2\times 2}^l$ fulfilling $u_{2\times 2}^l = \sigma_{2\times 2}^l \sigma_{2\times 2}^{lT}$, where $\sigma_{2\times 2}^l$ is a two-dimensional unitary matrix. As a result, the matrix $\Sigma_{l1}^\dagger X_l \Sigma_{l1}^*$ can be written into

$$\Sigma_{l1}^\dagger X_l \Sigma_{l1}^* = \begin{pmatrix} e^{i\xi_1/2} & 0 \\ 0 & \sigma_{2\times 2}^l \end{pmatrix} \begin{pmatrix} e^{i\xi_1/2} & 0 \\ 0 & \sigma_{2\times 2}^{lT} \end{pmatrix}. \quad (2.10)$$

Then, we can obtain the Takagi factorization of X_l as

$$X_l = \left[\Sigma_{l1} \begin{pmatrix} e^{i\xi_1/2} & 0 \\ 0 & \sigma_{2\times 2}^l \end{pmatrix} \right] \left[\Sigma_{l1} \begin{pmatrix} e^{i\xi_1/2} & 0 \\ 0 & \sigma_{2\times 2}^l \end{pmatrix} \right]^T$$
$$\equiv \Sigma_l \Sigma_l^T \quad (2.11)$$

with

$$\Sigma_l = \Sigma_{l1} \begin{pmatrix} e^{i\xi_1/2} & 0 \\ 0 & \sigma_{2\times 2}^l \end{pmatrix}. \quad (2.12)$$

It is straightforward to check that the remnant flavor transformation $\rho_3(g_l)$ is diagonalized by Σ_l,

$$\Sigma_l^\dagger \rho_3(g_l) \Sigma_l = \text{diag}(1, -1, -1). \quad (2.13)$$

From Eq. (2.2a), we can obtain that the constraint on the unitary transformation U_l from the residual CP transformation X_l is

$$U_l^\dagger X_l U_l^* = \text{diag}(e^{i\beta_e}, e^{i\beta_\mu}, e^{i\beta_\tau}) \equiv Q_l^2, \quad (2.14)$$

where $\beta_{e,\mu,\tau}$ are arbitrary real parameters. Thus, we have

$$U_l^\dagger \Sigma_l \Sigma_l^T U_l^* = Q_l^2, \quad (2.15)$$

which leads to

$$(\Sigma_l^T U_l^* Q_l^{-1})^T (\Sigma_l^T U_l^* Q_l^{-1}) = 1. \quad (2.16)$$

Hence, the combination $\Sigma_l^T U_l^* Q_l^{-1}$ is an orthogonal matrix, and it is also a unitary matrix. Therefore, $\Sigma_l^T U_l^* Q_l^{-1}$ is a real orthogonal matrix denoted by $O_{3\times 3}$. Then, the unitary transformation U_l takes the following form:

$$U_l = \Sigma_l O_{3\times 3} Q_l^{-1}. \quad (2.17)$$

Furthermore, Eq. (2.2b) implies that U_l is also subject to the constraint of the residual flavor symmetry as follows,

$$U_l^\dagger \rho_3(g_l) U_l = P_l \text{diag}(1, -1, -1) P_l^T, \quad (2.18)$$

where P_l is a generic permutation matrix, and it can take six possible forms, 1, P_{12}, P_{13}, P_{23}, $P_{23}P_{12}$, and $P_{23}P_{13}$ with

$$P_{12} = \begin{pmatrix} 0 & 1 & 0 \\ 1 & 0 & 0 \\ 0 & 0 & 1 \end{pmatrix}, \qquad P_{13} = \begin{pmatrix} 0 & 0 & 1 \\ 0 & 1 & 0 \\ 1 & 0 & 0 \end{pmatrix},$$

$$P_{23} = \begin{pmatrix} 1 & 0 & 0 \\ 0 & 0 & 1 \\ 0 & 1 & 0 \end{pmatrix}. \quad (2.19)$$

Plugging the expression of U_l in Eq. (2.17) into Eq. (2.18), we obtain

$$P_l^T Q_l O_{3\times 3}^\dagger \Sigma_l^\dagger \rho_3(g_l) \Sigma_l O_{3\times 3} Q_l^{-1} P_l = \text{diag}(1, -1, -1). \quad (2.20)$$

Using Eq. (2.13), we have

$$[O_{3\times3}Q_l^{-1}P_l]^\dagger \mathrm{diag}(1,-1,-1)[O_{3\times3}Q_l^{-1}P_l]$$
$$= \mathrm{diag}(1,-1,-1). \qquad (2.21)$$

Therefore, the combination $O_{3\times3}Q_l^{-1}P_l$ is a block diagonal unitary matrix, and it can be parametrized as

$$O_{3\times3}Q_l^{-1}P_l = \begin{pmatrix} e^{i\xi_2} & 0 \\ 0 & v_{2\times2}^l \end{pmatrix}, \qquad (2.22)$$

where ξ_2 is a real number and $v_{2\times2}^l$ is a two-dimensional unitary matrix. Thus, we have

$$(O_{3\times3}Q_l^{-1}P_l)^T (O_{3\times3}Q_l^{-1}P_l) = P_l^T Q_l^{-2} P_l$$
$$= \begin{pmatrix} e^{2i\xi_2} & 0 \\ 0 & v_{2\times2}^{lT} v_{2\times2}^l \end{pmatrix}, \qquad (2.23)$$

which implies

$$\left[\begin{pmatrix} e^{i\xi_2} & 0 \\ 0 & v_{2\times2}^l \end{pmatrix} P_l^T Q_l P_l \right]^T \left[\begin{pmatrix} e^{i\xi_2} & 0 \\ 0 & v_{2\times2}^l \end{pmatrix} P_l^T Q_l P_l \right] = 1. \qquad (2.24)$$

Hence, $\begin{pmatrix} e^{i\xi_2} & 0 \\ 0 & v_{2\times2}^l \end{pmatrix} P_l^T Q_l P_l$ is a block diagonal real orthogonal matrix, and it takes the form

$$\begin{pmatrix} e^{i\xi_2} & 0 \\ 0 & v_{2\times2}^l \end{pmatrix} P_l^T Q_l P_l = S_{23}^T(\theta_l), \qquad (2.25)$$

where $S_{23}(\theta_l)$ is a rotation matrix with

$$S_{23}(\theta_l) \equiv \begin{pmatrix} 1 & 0 & 0 \\ 0 & \cos\theta_l & \sin\theta_l \\ 0 & -\sin\theta_l & \cos\theta_l \end{pmatrix}. \qquad (2.26)$$

As a consequence, the unitary transformation U_l is fixed by the residual symmetry $Z_2 \times CP$ to be

$$U_l = \Sigma_l S_{23}^T(\theta_l) P_l^T Q_l^{-1}. \qquad (2.27)$$

Hence, the unitary transformation U_l can be easily obtained by determining the Takagi factorization matrix Σ_l. Notice that if Σ_l is a Takagi factorization of X_l, $\Sigma_l S_{23}(\theta_l')$ is also a valid Takagi factorization fulfilling Eq. (2.13), where $S_{23}(\theta_l')$ is an arbitrary rotation in the (23)-plane and it can be absorbed into $S_{23}(\theta_l)$ through parameter redefinition. As a consequence, the result for U_l in Eq. (2.27) is not changed. Similarly, the residual flavor symmetry of the neutrino mass matrix is denoted as $Z_2^{g_\nu} \equiv \{1, g_\nu\}$ with $g_\nu^2 = 1$, the residual

CP transformation is X_ν, and CP should commute with $Z_2^{g_\nu}$ as well,

$$X_\nu \rho_{\mathbf{3}}^*(g_\nu) X_\nu^{-1} = \rho_{\mathbf{3}}(g_\nu). \qquad (2.28)$$

The invariance of the neutrino mass matrix under the residual symmetry $Z_2^{g_\nu} \times X_\nu$ requires [24,39]

$$\rho_{\mathbf{3}}^T(g_\nu) m_\nu \rho_{\mathbf{3}}(g_\nu) = m_\nu, \qquad X_\nu^T m_\nu X_\nu = m_\nu^*. \qquad (2.29)$$

Plugging $U_\nu^T m_\nu U_\nu = \mathrm{diag}(m_1, m_2, m_3)$ into this equation, we can derive the following constraints on the unitary transformation U_ν,

$$U_\nu^\dagger \rho_{\mathbf{3}}(g_\nu) U_\nu = \mathrm{diag}(\pm1, \pm1, \pm1), \qquad (2.30a)$$

$$U_\nu^\dagger X_\nu U_\nu^* = \mathrm{diag}(\pm1, \pm1, \pm1) \equiv Q_\nu^2, \qquad (2.30b)$$

where Q_ν is a diagonal and unitary matrix with nonvanishing entries equal to ±1 and $\pm i$. Without loss of generality, Q_ν can be parametrized as

$$Q_\nu = \begin{pmatrix} 1 & 0 & 0 \\ 0 & i^{k_1} & 0 \\ 0 & 0 & i^{k_2} \end{pmatrix}, \qquad (2.31)$$

with $k_{1,2} = 0, 1, 2, 3$. First, we can diagonalize the residual flavor symmetry transformation $\rho_{\mathbf{3}}(g_\nu)$ by a unitary transformation $\Sigma_{\nu1}$ as

$$\Sigma_{\nu1}^\dagger \rho_{\mathbf{3}}(g_\nu) \Sigma_{\nu1} = \hat\rho_{\mathbf{3}}(g_\nu) = \mathrm{diag}(1,-1,-1). \qquad (2.32)$$

The consistency condition of remnant symmetry is [24,39]

$$X_\nu \rho_{\mathbf{3}}^*(g_\nu) X_\nu^\dagger = \rho_{\mathbf{3}}(g_\nu^{-1}) = \rho_{\mathbf{3}}(g_\nu), \qquad (2.33)$$

which leads to

$$X_\nu \Sigma_{\nu1}^* \hat\rho_{\mathbf{3}}^*(g_\nu) \Sigma_{\nu1}^T X_\nu^\dagger = \Sigma_{\nu1} \hat\rho_{\mathbf{3}}(g_\nu) \Sigma_{\nu1}^\dagger. \qquad (2.34)$$

Thus, we have

$$(\Sigma_{\nu1}^\dagger X_\nu \Sigma_{\nu1}^*) \hat\rho_{\mathbf{3}}^*(g_\nu) (\Sigma_{\nu1}^\dagger X_\nu \Sigma_{\nu1}^*)^\dagger = \hat\rho_{\mathbf{3}}(g_\nu). \qquad (2.35)$$

Hence, $\Sigma_{\nu1}^\dagger X_\nu \Sigma_{\nu1}^*$ is a block diagonal matrix, and it is of the following form,

$$\Sigma_{\nu1}^\dagger X_\nu \Sigma_{\nu1}^* = \begin{pmatrix} e^{i\zeta_1} & 0 \\ 0 & u_{2\times2}^\nu \end{pmatrix}, \qquad (2.36)$$

where ζ_1 is an arbitrary real number and $u_{2\times2}^\nu$ is a two-dimensional symmetric unitary matrix. $u_{2\times2}^\nu$ can be factorized into the form $u_{2\times2}^\nu = \sigma_{2\times2}^\nu \sigma_{2\times2}^{\nu T}$ with $\sigma_{2\times2}^\nu \sigma_{2\times2}^{\nu\dagger} = 1$. Then, we obtain

$$\Sigma_{\nu1}^\dagger X_\nu \Sigma_{\nu1}^* = \Sigma_{\nu2}\Sigma_{\nu2}^T, \qquad (2.37)$$

where

$$\Sigma_{\nu2} = \begin{pmatrix} e^{i\zeta_1/2} & 0 \\ 0 & \sigma_{2\times2}^\nu \end{pmatrix}. \qquad (2.38)$$

As a consequence, the Takagi factorization of the residual CP transformation X_ν is given by

$$X_\nu = \Sigma_\nu \Sigma_\nu^T \qquad (2.39)$$

with $\Sigma_\nu = \Sigma_{\nu1}\Sigma_{\nu2}$. It is easy to check that the residual flavor transformation $\rho_{\mathbf{3}}(g_\nu)$ is diagonalized by Σ_ν as well,

$$\begin{aligned} \Sigma_\nu^\dagger \rho_{\mathbf{3}}(g_\nu)\Sigma_\nu &= \Sigma_{\nu2}^\dagger\Sigma_{\nu1}^\dagger\rho_{\mathbf{3}}(g_\nu)\Sigma_{\nu1}\Sigma_{\nu2} \\ &= \Sigma_{\nu2}^\dagger \mathrm{diag}(1,-1,-1)\Sigma_{\nu2} \\ &= \mathrm{diag}(1,-1,-1). \end{aligned} \qquad (2.40)$$

Now, we proceed to discuss the constraint on U_ν from the remnant CP transformation. Substituting the relation $X_\nu = \Sigma_\nu\Sigma_\nu^T$ into Eq. (2.30b), we get

$$(Q_\nu U_\nu^\dagger\Sigma_\nu)(Q_\nu U_\nu^\dagger\Sigma_\nu)^T = 1. \qquad (2.41)$$

This implies that $Q_\nu U_\nu^\dagger\Sigma_\nu$ is a real orthogonal matrix denoted as $O_{3\times3}$. Therefore, the unitary transformation U_ν is of the form

$$U_\nu = \Sigma_\nu O_{3\times3}^T Q_\nu. \qquad (2.42)$$

Subsequently, we consider the constraint from the residual flavor symmetry given in Eq. (2.30a),

$$U_\nu^\dagger\rho_{\mathbf{3}}(g_\nu)U_\nu = P_\nu^T\mathrm{diag}(1,-1,-1)P_\nu, \qquad (2.43)$$

where P_ν is a permutation matrix, since the neutrino masses are unconstrained in the present framework and the neutrino mass spectrum can be either normal hierarchy (NH) or inverted hierarchy (IH). Inserting Eq. (2.42) into Eq. (2.43), one finds

$$\begin{aligned} Q_\nu^{-1}O_{3\times3}\Sigma_\nu^\dagger\rho_{\mathbf{3}}(g_\nu)\Sigma_\nu O_{3\times3}^T Q_\nu \\ = Q_\nu^{-1}O_{3\times3}\mathrm{diag}(1,-1,-1)O_{3\times3}^T Q_\nu \\ = P_\nu^T\mathrm{diag}(1,-1,-1)P_\nu, \end{aligned} \qquad (2.44)$$

which gives rise to

$$\mathrm{diag}(1,-1,-1)(O_{3\times3}^T Q_\nu P_\nu^T) = (O_{3\times3}^T Q_\nu P_\nu^T)\mathrm{diag}(1,-1,-1). \qquad (2.45)$$

Therefore, $O_{3\times3}^T Q_\nu P_\nu^T$ is a block-diagonal unitary matrix, and we can parametrize it as

$$O_{3\times3}^T Q_\nu P_\nu^T = \begin{pmatrix} e^{i\zeta_2} & 0 \\ 0 & v_{2\times2}^\nu \end{pmatrix}, \qquad (2.46)$$

where ζ_2 is real and $v_{2\times2}^\nu$ is a two-dimensional unitary matrix. Both sides of this equation multiply with their transpose, and we obtain

$$\begin{aligned} (O_{3\times3}^T Q_\nu P_\nu^T)^T(O_{3\times3}^T Q_\nu P_\nu^T) &= P_\nu Q_\nu^2 P_\nu^T \\ &= \begin{pmatrix} e^{2i\zeta_2} & 0 \\ 0 & v_{2\times2}^{\nu T}v_{2\times2}^\nu \end{pmatrix}, \end{aligned} \qquad (2.47)$$

which implies

$$\left[\begin{pmatrix} e^{i\zeta_2} & 0 \\ 0 & v_{2\times2}^\nu \end{pmatrix}P_\nu Q_\nu^{-1}P_\nu^T\right]^T\left[\begin{pmatrix} e^{i\zeta_2} & 0 \\ 0 & v_{2\times2}^\nu \end{pmatrix}P_\nu Q_\nu^{-1}P_\nu^T\right] = 1. \qquad (2.48)$$

Therefore, $\begin{pmatrix} e^{i\zeta_2} & 0 \\ 0 & v_{2\times2}^\nu \end{pmatrix}P_\nu Q_\nu^{-1}P_\nu^T$ is a block-diagonal real orthogonal matrix, and it is of the following form,

$$\begin{pmatrix} e^{i\zeta_2} & 0 \\ 0 & v_{2\times2}^\nu \end{pmatrix}P_\nu Q_\nu^{-1}P_\nu^T = S_{23}(\theta_\nu), \qquad (2.49)$$

where θ_ν is real. Consequently, the unitary transformation U_ν is fixed to be

$$U_\nu = \Sigma_\nu S_{23}(\theta_\nu)P_\nu Q_\nu. \qquad (2.50)$$

The lepton mixing matrix U_{PMNS} is a result of the mismatch between U_l and U_ν. Hence, we find U_{PMNS} is of the form

$$U_{\mathrm{PMNS}} = U_l^\dagger U_\nu = Q_l P_l S_{23}(\theta_l)\Sigma_l^\dagger\Sigma_\nu S_{23}(\theta_\nu)P_\nu Q_\nu, \qquad (2.51)$$

where the phase matrix Q_l can be absorbed by redefinition of the charged lepton fields. We see that the lepton mixing matrix depends on two free continuous parameters θ_l and θ_ν, and one entry of the PMNS matrix is fixed to be some constant value by the postulated residual symmetry. Notice that $S_{23}(\theta+\pi) = S_{23}(\theta)\mathrm{diag}(1,-1,-1) = \mathrm{diag}(1,-1,-1)S_{23}(\theta)$ where the diagonal matrix can be absorbed into the matrices Q_l and Q_ν, and consequently the fundamental interval of the parameters θ_l and θ_ν is $[0,\pi)$.

If two pairs of residual subgroups $\{Z_2^{g_l'} \times X_l', Z_2^{g_\nu'} \times X_\nu'\}$ and $\{Z_2^{g_l} \times X_l, Z_2^{g_\nu} \times X_\nu\}$ are related by a similarity transformation

$$hg_l h^{-1} = g'_l, \qquad \rho_3(h) X_l \rho_3(h)^T = X'_l,$$
$$hg_\nu h^{-1} = g'_\nu, \qquad \rho_3(h) X_\nu \rho_3(h)^T = X'_\nu \qquad (2.52)$$

with $h \in S_4$, then the unitary transformations of the changed lepton and neutrino fields are related by

$$U'_l = \rho_3(h) U_l, \qquad U'_\nu = \rho_3(h) U_\nu. \qquad (2.53)$$

Therefore, the same result for the PMNS matrix would be obtained.

B. Criterion for the equivalence of two mixing patterns

In some cases, two distinct residual symmetries lead to the same mixing pattern, if a possible shift in the continuous free parameters θ_l and θ_ν is taken into account. Then, we shall call these two mixing patterns are equivalent. In this section, we shall derive the criterion to determine whether two resulting mixing patterns are equivalent or not. In our approach, the lepton mixing matrices derived from two generic residual symmetries take the form

$$U_{\mathrm{PMNS}} = Q_l P_l S_{23}(\theta_l) \Sigma_l^\dagger \Sigma_\nu S_{23}(\theta_\nu) P_\nu Q_\nu, \qquad (2.54)$$

$$U'_{\mathrm{PMNS}} = Q'_l P'_l S_{23}(\theta'_l) \Sigma_l'^\dagger \Sigma'_\nu S_{23}(\theta'_\nu) P'_\nu Q'_\nu. \qquad (2.55)$$

Obviously, the fixed element has to be equal if the two mixing patterns are equivalent, and without loss of generality, we assume it is the (11) entry of the PMNS matrix. As a result, the permutation matrices P_l, P_ν, P'_l, and P'_ν can only be 1 and P_{23}. Because the identities

$$P_{23} S_{23}(\theta_l) = \mathrm{diag}(1, -1, 1) S_{23}(\theta_l - \pi/2),$$
$$S_{23}(\theta_\nu) P_{23} = S_{23}(\theta_\nu + \pi/2) \mathrm{diag}(1, -1, 1) \qquad (2.56)$$

are satisfied, and the diagonal matrix can be absorbed into the matrices Q_l and Q_ν, we could choose $P_l = P_\nu = P'_l = P'_\nu = 1$. For any given values of θ_l and θ_ν and the matrices Q_l, P_l, Q_ν, and P_ν, if the corresponding solutions of θ'_l and θ'_ν as well as Q'_l, P'_l, Q'_ν, and P'_ν can be found such that the equality $U_{\mathrm{PMNS}} = U'_{\mathrm{PMNS}}$ is fulfilled, these two mixing patterns would be equivalent, i.e.,

$$Q_l S_{23}(\theta_l) U S_{23}(\theta_\nu) Q_\nu = Q'_l S_{23}(\theta'_l) U' S_{23}(\theta'_\nu) Q'_\nu, \qquad (2.57)$$

where $U \equiv \Sigma_l^\dagger \Sigma_\nu$ and $U' \equiv \Sigma_l'^\dagger \Sigma'_\nu$. Then, we have

$$Q_L S_{23}(\theta_l) U S_{23}(\theta_\nu) Q_N = S_{23}(\theta'_l) U' S_{23}(\theta'_\nu), \qquad (2.58)$$

where $Q_L = Q_l'^\dagger Q_l$ is a generic diagonal phase matrix and $Q_N = Q_\nu Q_\nu'^\dagger$ is also diagonal with entries ± 1 and $\pm i$. The matrices on both sides of Eq. (2.58) multiplying with their transpose leads to

$$Q_L S_{23}(\theta_l) U S_{23}(\theta_\nu) Q_N^2 S_{23}^T(\theta_\nu) U^T S_{23}^T(\theta_l) Q_L$$
$$= S_{23}(\theta'_l) U' U'^T S_{23}^T(\theta'_l). \qquad (2.59)$$

Subsequently, taking the trace, we obtain

$$\mathrm{Tr}[S_{23}^T(\theta_l) Q_L^2 S_{23}(\theta_l) U S_{23}(\theta_\nu) Q_N^2 S_{23}^T(\theta_\nu) U^T] = \mathrm{Tr}[U' U'^T]. \qquad (2.60)$$

Since the right-hand side of this equality is a constant and it does not depend on θ_l and θ_ν, the phase matrices Q_L and Q_N should be of the form

$$Q_L = \begin{pmatrix} e^{i\delta_1} & 0 & 0 \\ 0 & e^{i\delta_2} & 0 \\ 0 & 0 & k_1 e^{i\delta_2} \end{pmatrix},$$
$$Q_N = \begin{pmatrix} \eta_1 & 0 & 0 \\ 0 & \eta_2 & 0 \\ 0 & 0 & k_2 \eta_2 \end{pmatrix}, \qquad (2.61)$$

where $k_{1,2} = \pm 1$, $\delta_{1,2}$ are real parameters and $\eta_{1,2}$ are ± 1 and $\pm i$ with $e^{i\delta_1} \eta_1 = 1$. Thus, from Eq. (2.58), we can derive

$$Q_L U Q_N = S_{23}(\theta''_l) U' S_{23}(\theta''_\nu), \qquad (2.62)$$

with

$$\theta''_l = \theta'_l - k_1 \theta_l, \quad \theta''_\nu = \theta'_\nu - k_2 \theta_\nu. \qquad (2.63)$$

Once the residual symmetries are specified, the unitary matrices U and U' can be determined by following the procedures listed in Sec. II A. Generically, U and U' can be written as

$$U = \begin{pmatrix} a_1 & a_2 & a_3 \\ a_4 & a_5 & a_6 \\ a_7 & a_8 & a_9 \end{pmatrix}, \quad U' = \begin{pmatrix} b_1 & b_2 & b_3 \\ b_4 & b_5 & b_6 \\ b_7 & b_8 & b_9 \end{pmatrix}. \qquad (2.64)$$

A necessary condition for the equivalence of U_{PMNS} and U'_{PMNS} is $a_1 = b_1$, which cannot be 0 or 1 in order to be compatible with experimental data. First, let us consider a special case with

$$Q_L = \begin{pmatrix} 1 & 0 & 0 \\ 0 & e^{i\delta} & 0 \\ 0 & 0 & e^{i\delta} \end{pmatrix}, \quad Q_N = \begin{pmatrix} 1 & 0 & 0 \\ 0 & 1 & 0 \\ 0 & 0 & 1 \end{pmatrix}. \qquad (2.65)$$

Solving Eq. (2.62) for the variables θ''_l, θ''_ν, and δ, we can obtain the condition for the existence of a solution:

(i) $b_2^2 + b_3^2 \neq 0, b_4^2 + b_7^2 \neq 0$:

In this case, the solutions for θ_l'', θ_ν'', and δ are given by

$$\cos\theta_l'' = \frac{a_4 b_4 + a_7 b_7}{b_4^2 + b_7^2} e^{i\delta}, \quad \sin\theta_l'' = \frac{a_4 b_7 - a_7 b_4}{b_4^2 + b_7^2} e^{i\delta},$$

$$e^{-2i\delta} = \frac{a_4^2 + a_7^2}{b_4^2 + b_7^2},$$

$$\cos\theta_\nu'' = \frac{a_2 b_2 + a_3 b_3}{b_2^2 + b_3^2}, \quad \sin\theta_\nu'' = \frac{a_3 b_2 - a_2 b_3}{b_2^2 + b_3^2}.$$

$$(2.66)$$

Since θ_l'', θ_ν'', and δ are real parameters, a_i and b_i should be subject to the following constraints:

$$(a_4 b_4 + a_7 b_7)(a_4^* b_7^* - a_7^* b_4^*) \in \mathbb{R},$$
$$|a_4^2 + a_7^2| = |b_4^2 + b_7^2|,$$
$$(a_2 b_2 + a_3 b_3)(a_2^* b_3^* - a_3^* b_2^*) \in \mathbb{R},$$
$$a^2 + a_3^2 = b_2^2 + b_3^2. \qquad (2.67)$$

Inserting Eq. (2.66) into Eq. (2.62), we find that the equivalence of these two mixing patterns requires

$$a_5 = \frac{(xb_5 + yb_6)z + (xb_8 + yb_9)w}{(b_2^2 + b_3^2)(b_4^2 + b_7^2)},$$

$$a_6 = \frac{(xb_6 - yb_5)z + (xb_9 - yb_8)w}{(b_2^2 + b_3^2)(b_4^2 + b_7^2)},$$

$$a_8 = \frac{(xb_8 + yb_9)z - (xb_5 + yb_6)w}{(b_2^2 + a_3^2)(b_4^2 + b_7^2)},$$

$$a_9 = \frac{(xb_9 - yb_8)z - (xb_6 - yb_5)w}{(b_2^2 + b_3^2)(b_4^2 + b_7^2)}, \qquad (2.68)$$

with

$$x = a_2 b_2 + a_3 b_3, \qquad y = a_2 b_3 - a_3 b_2,$$
$$z = a_4 b_4 + a_7 b_7, \qquad w = a_4 b_7 - a_7 b_4. \qquad (2.69)$$

(ii) $b_2^2 + b_3^2 = 0, b_4^2 + b_7^2 \neq 0$:

This case requires

$$b_3 = is_1 b_2, \quad a_3 = is_1 a_2, \quad \text{with } s_1 = \pm 1. \quad (2.70)$$

The parameters θ_l'', θ_ν'', and δ are determined to be

$$\cos\theta_l'' = \frac{a_4 b_4 + a_7 b_7}{b_4^2 + b_7^2} e^{i\delta}, \quad \sin\theta_l'' = \frac{a_4 b_7 - a_7 b_4}{b_4^2 + b_7^2} e^{i\delta},$$

$$e^{-2i\delta} = \frac{a_4^2 + a_7^2}{b_4^2 + b_7^2},$$

$$\cos\theta_\nu'' = \Re(a_2/b_2), \quad \sin\theta_\nu'' = -s_1 \Im(a_2/b_2),$$

$$(2.71)$$

with the constraints

$$(a_4 b_4 + a_7 b_7)(a_4^* b_7^* - a_7^* b_4^*) \in \mathbb{R},$$
$$|a_4^2 + a_7^2| = |b_4^2 + b_7^2|. \qquad (2.72)$$

These two PMNS matrices would be equivalent if and only if the following conditions are fulfilled:

$$a_5(b_4^2 + b_7^2) = s_1(zb_6 + wb_9)\Im(a_2/b_2)$$
$$+ (zb_5 + wb_8)\Re(a_2/b_2),$$

$$a_6(b_4^2 + b_7^2) = -s_1(zb_5 + wb_8)\Im(a_2/b_2)$$
$$+ (zb_6 + wb_9)\Re(a_2/b_2),$$

$$a_8(b_4^2 + b_7^2) = s_1(zb_9 - wb_6)\Im(a_2/b_2)$$
$$+ (zb_8 - wb_5)\Re(a_2/b_2),$$

$$a_9(b_4^2 + b_7^2) = -s_1(zb_8 - wb_5)\Im(a_2/b_2)$$
$$+ (zb_9 - wb_6)\Re(a_2/b_2). \qquad (2.73)$$

(iii) $b_2^2 + b_3^2 \neq 0, b_4^2 + b_7^2 = 0$:

From $b_4^2 + b_7^2 = 0$, we obtain $b_7 = is_2 b_4$ with $s_2 = \pm 1$. Moreover, the equality $a_7 = is_2 a_4$ should be satisfied; otherwise, U_{PMNS} and U'_{PMNS} are two different mixing patterns. The condition of equivalence in Eq. (2.62) gives rise to

$$t_i T_j - t_j T_i = 0, \quad t_i/T_i \in \mathbb{R}, \text{ with } i,j = 5,6,8,9,$$
$$(2.74)$$

where

$$t_5 = za_5 - wb_5 - vb_6,$$
$$t_6 = za_6 - wb_6 + vb_5,$$
$$t_8 = -za_8 + wb_8 + vb_9,$$
$$t_9 = -za_9 + wb_9 - vb_8,$$
$$T_5 = -iza_5 + s_2(wb_8 + vb_9),$$
$$T_6 = -iza_6 + s_2(wb_9 - vb_8),$$
$$T_8 = iza_8 + s_2(wb_5 + vb_6),$$
$$T_9 = iza_9 + s_2(wb_6 - vb_5), \qquad (2.75)$$

and

$$z \equiv b_4(b_2^2 + b_3^2),$$
$$w \equiv a_4(a_2b_2 + a_3b_3),$$
$$v \equiv a_4(a_2b_3 - a_3b_2). \tag{2.76}$$

The values of the rotation angles θ_l'' and θ_ν'' are

$$\cos\theta_l'' = \Re(a_4 e^{i\delta}/b_4), \qquad \sin\theta_l'' = s_2\Im(a_4 e^{i\delta}/b_4),$$
$$\cos\theta_\nu'' = \frac{a_2b_2 + a_3b_3}{b_2^2 + b_3^2}, \qquad \sin\theta_\nu'' = \frac{a_3b_2 - a_2b_3}{b_2^2 + b_3^2}, \tag{2.77}$$

with the constraints

$$(a_2b_2 + a_3b_3)(a_2^* b_3^* - a_3^* b_2^*) \in \mathbb{R},$$
$$a_2^2 + a_3^2 = b_2^2 + b_3^2. \tag{2.78}$$

The phase δ is determined by

$$\frac{\Im(a_4 e^{i\delta}/b_4)}{\Re(a_4 e^{i\delta}/b_4)} = \frac{t_i}{T_i}. \tag{2.79}$$

(iv) $b_2^2 + b_3^2 = 0, b_4^2 + b_7^2 = 0$:
In the same fashion as in previous cases, we find

$$b_3 = is_3 b_2, \quad a_3 = is_3 a_2, \quad s_3 = \pm 1,$$
$$b_7 = is_4 b_4, \quad a_7 = is_4 a_4, \quad s_4 = \pm 1. \tag{2.80}$$

The condition of equivalence in Eq. (2.62) would be fulfilled if

$$t_i' T_j' - t_j' T_i' = 0, \quad t_i'/T_i' \in \mathbb{R}, \quad \text{with } i,j = 5,6,8,9, \tag{2.81}$$

where

$$t_5' = a_5 b_4 - a_4[s_3 b_6 \Im(a_2/b_2) + b_5 \Re(a_2/b_2)],$$
$$t_6' = a_6 b_4 + a_4[s_3 b_5 \Im(a_2/b_2) - b_6 \Re(a_2/b_2)],$$
$$t_8' = a_8 b_4 - a_4[s_3 b_9 \Im(a_2/b_2) + b_8 \Re(a_2/b_2)],$$
$$t_9' = a_9 b_4 + a_4[s_3 b_8 \Im(a_2/b_2) - b_9 \Re(a_2/b_2)],$$
$$T_5' = -ia_5 b_4 + s_4 a_4[s_3 b_9 \Im(a_2/b_2) + b_8 \Re(a_2/b_2)],$$
$$T_6' = -ia_6 b_4 - s_4 a_4[s_3 b_8 \Im(a_2/b_2) - b_9 \Re(a_2/b_2)],$$
$$T_8' = -ia_8 b_4 - s_4 a_4[s_3 b_6 \Im(a_2/b_2) + b_5 \Re(a_2/b_2)],$$
$$T_9' = -ia_9 b_4 + s_4 a_4[s_3 b_5 \Im(a_2/b_2) - b_6 \Re(a_2/b_2)]. \tag{2.82}$$

The solutions for θ_l'', θ_ν'', and δ are

$$\cos\theta_l'' = \Re(a_4 e^{i\delta}/b_4), \qquad \sin\theta_l'' = s_4\Im(a_4 e^{i\delta}/b_4),$$
$$\frac{\Im(a_4 e^{i\delta}/b_4)}{\Re(a_4 e^{i\delta}/b_4)} = \frac{t_i'}{T_i'},$$
$$\cos\theta_\nu'' = \Re(a_2/b_2), \qquad \sin\theta_\nu'' = -s_3\Im(a_2/b_2). \tag{2.83}$$

For the most general values of the diagonal matrices Q_L and Q_N,

$$Q_L = \begin{pmatrix} \eta_1^{-1} & 0 & 0 \\ 0 & e^{i\delta} & 0 \\ 0 & 0 & k_1 e^{i\delta} \end{pmatrix},$$
$$Q_N = \begin{pmatrix} \eta_1 & 0 & 0 \\ 0 & \eta_2 & 0 \\ 0 & 0 & k_2\eta_2 \end{pmatrix}, \tag{2.84}$$

the condition for the equivalence of two generic mixing patterns can be obtained from the above results by making the following substitutions:

$$a_1 \to a_1, \qquad a_2 \to \eta_1^{-1}\eta_2 a_2, \qquad a_3 \to k_2\eta_1^{-1}\eta_2 a_3,$$
$$a_4 \to \eta_1 a_4, \qquad a_5 \to \eta_2 a_5, \qquad a_6 \to k_2\eta_2 a_6,$$
$$a_7 \to k_1\eta_1 a_7, \qquad a_8 \to k_1\eta_2 a_8, \qquad a_9 \to k_1 k_2\eta_2 a_9. \tag{2.85}$$

C. Possible mixing patterns from S_4 and CP and numerical results

We shall perform a comprehensive study of the lepton mixing patterns arising from the breaking of S_4 and CP symmetry into two distinct residual groups of the structure $Z_2 \times CP$ in the charged lepton and neutrino sectors. The basic properties of the S_4 group and its representation are collected in Appendix A. It turns out that the most general CP transformation compatible with S_4 is of the same form as the flavor symmetry transformation in our chosen basis [39,42]. Each of the nine different Z_2 symmetries in Eq. (A3) together with the compatible CP transformation can be residual symmetry of the neutrino and charged lepton mass matrices.

By applying the similarity transformation and the equivalence criterion derived in Sec. II B, we find that it is sufficient to only consider a number of independent cases which lead to different results for mixing angles and CP phases. All possible permutations of the rows and columns of the mixing matrix would be considered. We exclude all patterns that can not describe the experimental data on lepton mixing angles at the 3σ level for certain values of the

free parameters θ_l and θ_ν. As a result, we find in total 18 phenomenologically viable cases. The residual flavor symmetry of the neutrino and charged lepton sectors can be chosen to be $Z_2^{ST^2SU}$, Z_2^{TU}, or Z_2^S; the corresponding residual CP transformation X_r and the Takagi factorization matrix Σ are summarized in Table I. As shown in Sec. II A, the Takagi factorization Σ satisfies

$$X_r = \Sigma\Sigma^T, \qquad \Sigma^\dagger \rho_3(g_r)\Sigma = \text{diag}(1,-1,-1), \quad (2.86)$$

where g_r is the generator of G_r. Notice that $\rho_3(g_r)X_r$ is also a residual CP symmetry of the neutrino sector, and it leads to the same constraint on the neutrino mass matrix as X_r. For each possible residual symmetry, the lepton mixing matrix can be straightforwardly obtained by using the master formula of Eq. (2.51). If two cases possess the same residual symmetry but differ in the choice of the row permutation with $P_l = P_{12}$ and $P_l = P_{13}$ respectively, then the resulting mixing matrices are effectively related through the exchange of the second and the third rows, because the identity

TABLE I. The residual flavor symmetries $G_r = Z_2^{ST^2SU}$, Z_2^{TU}, Z_2^S and the corresponding residual CP transformations X_r consistent with G_r and the Takagi factorization matrix Σ. Let us denote the generator of G_r as g_r; then, $\rho_3(g_r)X_r$ is also a residual CP symmetry, and it is given in parentheses. For simplicity of notation, we do not distinguish between the abstract elements of the S_4 group and their representation matrices in **3**.

G_r	X_r	Σ
$Z_2^{ST^2SU}$	$T^2(TST^2U)$	$\frac{1}{\sqrt{6}}\begin{pmatrix} 2 & 0 & -\sqrt{2} \\ e^{\frac{i\pi}{3}} & \sqrt{3}e^{\frac{i\pi}{3}} & -\sqrt{2}e^{\frac{i\pi}{3}} \\ e^{-\frac{i\pi}{3}} & \sqrt{3}e^{-\frac{i\pi}{3}} & \sqrt{2}e^{-\frac{i\pi}{3}} \end{pmatrix}$
	$U(ST^2S)$	$\frac{1}{\sqrt{6}}\begin{pmatrix} 2i & \sqrt{2}i & 0 \\ -e^{-\frac{i\pi}{6}} & \sqrt{2}e^{-\frac{i\pi}{6}} & -\sqrt{3}e^{\frac{i\pi}{3}} \\ e^{\frac{i\pi}{6}} & -\sqrt{2}e^{\frac{i\pi}{6}} & \sqrt{3}e^{-\frac{i\pi}{3}} \end{pmatrix}$
Z_2^{TU}	$T(U)$	$\frac{1}{\sqrt{2}}\begin{pmatrix} 0 & 0 & \sqrt{2} \\ -e^{-\frac{i\pi}{3}} & e^{-\frac{i\pi}{3}} & 0 \\ e^{\frac{i\pi}{3}} & e^{\frac{i\pi}{3}} & 0 \end{pmatrix}$
	$STS(T^2STU)$	$\frac{1}{\sqrt{6}}\begin{pmatrix} 0 & 2i & \sqrt{2} \\ \sqrt{3}e^{\frac{i\pi}{6}} & e^{\frac{i\pi}{6}} & -\sqrt{2}e^{-\frac{i\pi}{3}} \\ \sqrt{3}e^{-\frac{i\pi}{6}} & -e^{-\frac{i\pi}{6}} & -\sqrt{2}e^{\frac{i\pi}{3}} \end{pmatrix}$
Z_2^S	$1(S)$	$\frac{1}{\sqrt{6}}\begin{pmatrix} \sqrt{2} & -1 & -\sqrt{3} \\ \sqrt{2} & 2 & 0 \\ \sqrt{2} & -1 & \sqrt{3} \end{pmatrix}$
	$SU(U)$	$\frac{1}{\sqrt{6}}\begin{pmatrix} \sqrt{2}i & 0 & -2 \\ \sqrt{2}i & -\sqrt{3}i & 1 \\ \sqrt{2}i & \sqrt{3}i & 1 \end{pmatrix}$
	$TST^2U(T^2STU)$	$\frac{1}{\sqrt{3}}\begin{pmatrix} 1 & i & 1 \\ 1 & e^{-\frac{i\pi}{6}} & -e^{-\frac{i\pi}{3}} \\ 1 & -e^{\frac{i\pi}{6}} & -e^{\frac{i\pi}{3}} \end{pmatrix}$

$$P_{23}P_{12}S_{23}(\theta) = \text{diag}(-1,1,1)P_{13}S_{23}(\theta - \pi/2) \quad (2.87)$$

is satisfied. Subsequently, we can extract the lepton mixing parameters, and the results for the mixing angles $\sin^2\theta_{13}$, $\sin^2\theta_{12}$, $\sin^2\theta_{23}$ and the CP invariants J_{CP}, I_1, and I_2 are listed in Tables II and III for all the viable cases. Here, J_{CP}, I_1, and I_2 are conventionally defined as [63,64]

$$J_{CP} = \Im(U_{\text{PMNS},11}U_{\text{PMNS},33}U_{\text{PMNS},13}^*U_{\text{PMNS},31}^*),$$
$$= \frac{1}{8}\sin 2\theta_{12}\sin 2\theta_{13}\sin 2\theta_{23}\cos\theta_{13}\sin\delta_{CP}, \quad (2.88)$$

$$I_1 = \Im(U_{\text{PMNS},12}^2 U_{\text{PMNS},11}^{*2})$$
$$= \sin^2\theta_{12}\cos^2\theta_{12}\cos^4\theta_{13}\sin\alpha_{21}, \quad (2.89)$$

$$I_2 = \Im(U_{\text{PMNS},13}^2 U_{\text{PMNS},11}^{*2})$$
$$= \sin^2\theta_{13}\cos^2\theta_{13}\cos^2\theta_{12}\sin(\alpha_{31} - 2\delta_{CP}), \quad (2.90)$$

where δ_{CP} is the Dirac CP-violating phase and α_{21} and α_{31} are the Majorana CP phases in the standard parametrization [65]. One notices that the invariants J_{CP}, I_1, and I_2 are exactly vanishing such that all three CP phases δ_{CP}, α_{21}, and α_{31} are trivial in some cases. Furthermore, we perform a conventional χ^2 analysis that includes the three mixing angles, and the results for the mixing parameters and the best fit values $(\theta_l, \theta_\nu)_{\text{bf}}$ are displayed in Tables IV, V, VI, and VII. For the residual flavor symmetry $(G_l, G_\nu) = (Z_2^{ST^2SU}, Z_2^{TU})$, one element of the PMNS matrix is fixed to be $1/2$. From Tables IV and V, we can see that the CP phases are predicted to be $\delta_{CP} \simeq 1.569\pi$, $\alpha_{21}(\text{mod }\pi) \simeq 0.728\pi$ and $\alpha_{31}(\text{mod }\pi) \simeq 0.808\pi$ in the case of $(X_l, X_\nu, P_l, P_\nu) = (T^2, T, P_{12}, P_{12})$, while all three CP phases are conserved for the remaining cases. In the same manner, for another residual flavor symmetry $(G_l, G_\nu) = (Z_2^{ST^2SU}, Z_2^S)$, the fixed element is $1/\sqrt{2}$, and we find that all that both Dirac and Majorana phases are trivial except $(X_l, X_\nu, P_l, P_\nu) = (T^2, SU, P_{12}, P_{13})$, $(T^2, SU, P_{12}, P_{13})$ which give rise to $\delta_{CP} \simeq 0.458\pi$, 0.542π, 1.458π or 1.542π. Moreover, the atmospheric mixing angle θ_{23} is predicted to be nonmaximal in all the cases studied. The latest results from T2K and NOνA show a weak evidence for a nearly maximal CP-violating phase $\delta_{CP} \sim 3\pi/2$ [66,67], and hits of $\delta_{CP} \sim 3\pi/2$ also show up in the global analysis of neutrino oscillation data [4–7]. On the other hand, NOνA excludes maximal mixing at 2.5σ, while the experimental data of T2K are consistent with maximal mixing [66,67]. Hence, the above mixing patterns predicting $\delta_{CP} \simeq 1.569\pi$, 1.458π, and 1.542π are slightly favored over the remaining cases by the present experimental data.

The numerical results listed in Tables IV, V, VI, and VII can be easily seen by plotting the contour regions of the mixing angle $\sin^2\theta_{ij}$ in the plane θ_ν vs θ_l, as shown in

TABLE II. Results of the mixing parameters for the independent and viable cases with $(G_l, G_\nu) = (Z_2^{ST^2SU}, Z_2^{TU})$. Note that the factors $(-1)^{k_1}$ and $(-1)^{k_2}$ are omitted in the expressions of I_1 and I_2 respectively, and they arise from the *CP* parity matrix $Q_\nu = \text{diag}(1, i^{k_1}, i^{k_2})$. For notational simplicity, here we introduce $\Delta_1 = \cos 2\theta_l(3 - 11\cos 2\theta_\nu) - 8\sqrt{2}\sin 2\theta_\nu \cos^2\theta_l + 12\sin 2\theta_l \sin\theta_\nu(\sqrt{2}\sin\theta_\nu + 2\cos\theta_\nu)$ and $\Delta_2 = \cos 2\theta_l(11\cos 2\theta_\nu - 3) - 8\sqrt{2}\sin 2\theta_\nu \sin^2\theta_l - 12\sin 2\theta_l \sin\theta_\nu(\sqrt{2}\sin\theta_\nu + 2\cos\theta_\nu)$.

$(G_l, G_\nu) = (Z_2^{ST^2SU}, Z_2^{TU})$		
(X_l, X_ν, P_l, P_ν)	$(U, T, P_{12}, 1)$	$(U, STS, P_{12}, 1)$
$\sin^2\theta_{13}$	$\frac{(\cos\theta_l(\sqrt{2}\sin\theta_\nu + 2\cos\theta_\nu) - 3\sin\theta_l\sin\theta_\nu)^2}{12}$	$\frac{(2\sin^2\theta_l\cos^2\theta_\nu + \sin^2\theta_\nu(\sin\theta_l - \sqrt{2}\cos\theta_l)^2)}{4}$
$\sin^2\theta_{12}$	$1 - \frac{6(2\sqrt{2}\sin 2\theta_l + \cos 2\theta_l + 3)}{\Delta_1 + 7\cos 2\theta_\nu + 33}$	$1 - \frac{2(2\sqrt{2}\sin 2\theta_l + \cos 2\theta_l + 3)}{4\sqrt{2}\sin 2\theta_l \sin^2\theta_\nu + \cos 2\theta_\nu + \cos 2\theta_l(3\cos 2\theta_\nu + 1) + 11}$
$\sin^2\theta_{23}$	$\frac{4(\sin\theta_\nu - 2\sqrt{2}\cos\theta_\nu)^2}{\Delta_1 + 7\cos 2\theta_\nu + 33}$	$\frac{2(\cos 2\theta_\nu + 3)}{4\sqrt{2}\sin 2\theta_l \sin^2\theta_\nu + \cos 2\theta_\nu + \cos 2\theta_l(3\cos 2\theta_\nu + 1) + 11}$
J_{CP}	0	$\frac{\sin 2\theta_\nu(\sin 2\theta_l - 2\sqrt{2}\cos 2\theta_l)}{32}$
I_1	0	$\frac{(\sin\theta_l - 3\sin 3\theta_l)\sin 2\theta_\nu(\sqrt{2}\sin\theta_l + 2\cos\theta_l)}{64}$
I_2	0	$-\frac{(\sin\theta_l - 3\sin 3\theta_l)\sin 2\theta_\nu(\sqrt{2}\sin\theta_l + 2\cos\theta_l)}{64}$
(X_l, X_ν, P_l, P_ν)	(U, T, P_{12}, P_{12})	(U, STS, P_{12}, P_{12})
$\sin^2\theta_{13}$	$\frac{(\cos\theta_l(\sqrt{2}\sin\theta_\nu + 2\cos\theta_\nu) - 3\sin\theta_l\sin\theta_\nu)^2}{12}$	$\frac{(2\sin^2\theta_l\cos^2\theta_\nu + \sin^2\theta_\nu(\sin\theta_l - \sqrt{2}\cos\theta_l)^2)}{4}$
$\sin^2\theta_{12}$	$\frac{12(\sin\theta_l + \sqrt{2}\cos\theta_l)^2}{\Delta_1 + 7\cos 2\theta_\nu + 33}$	$\frac{4(\sin\theta_l + \sqrt{2}\cos\theta_l)^2}{4\sqrt{2}\sin 2\theta_l \sin^2\theta_\nu + \cos 2\theta_\nu + \cos 2\theta_l(3\cos 2\theta_\nu + 1) + 11}$
$\sin^2\theta_{23}$	$\frac{4(\sin\theta_\nu - 2\sqrt{2}\cos\theta_\nu)^2}{\Delta_1 + 7\cos 2\theta_\nu + 33}$	$\frac{2(\cos 2\theta_\nu + 3)}{4\sqrt{2}\sin 2\theta_l \sin^2\theta_\nu + \cos 2\theta_\nu + \cos 2\theta_l(3\cos 2\theta_\nu + 1) + 11}$
J_{CP}	0	$\frac{\sin 2\theta_\nu(2\sqrt{2}\cos 2\theta_l - \sin 2\theta_l)}{32}$
I_1	0	$-\frac{(\sin\theta_l - 3\sin 3\theta_l)\sin 2\theta_\nu(\sqrt{2}\sin\theta_l + 2\cos\theta_l)}{64}$
I_2	0	$\frac{\sin\theta_l\sin 2\theta_\nu(\sqrt{2}(3\sin\theta_l + 7\sin 3\theta_l) - 14\cos\theta_l - 2\cos 3\theta_l)}{64}$
(X_l, X_ν, P_l, P_ν)	$(U, T, P_{13}, 1)$	$(U, STS, P_{13}, 1)$
$\sin^2\theta_{13}$	$\frac{(\sin\theta_l(\sqrt{2}\sin\theta_\nu + 2\cos\theta_\nu) + 3\sin\theta_\nu\cos\theta_l)^2}{12}$	$\frac{(2\cos^2\theta_l\cos^2\theta_\nu + \sin^2\theta_\nu(\cos\theta_l + \sqrt{2}\sin\theta_l)^2)}{4}$
$\sin^2\theta_{12}$	$1 + \frac{6(2\sqrt{2}\sin 2\theta_l + \cos 2\theta_l - 3)}{\Delta_2 + 7\cos 2\theta_\nu + 33}$	$1 - \frac{2(2\sqrt{2}\sin 2\theta_l + \cos 2\theta_l - 3)}{4\sqrt{2}\sin 2\theta_l \sin^2\theta_\nu - \cos 2\theta_\nu + \cos 2\theta_l(3\cos 2\theta_\nu + 1) - 11}$
$\sin^2\theta_{23}$	$1 - \frac{4(\sin\theta_\nu - 2\sqrt{2}\cos\theta_\nu)^2}{\Delta_2 + 7\cos 2\theta_\nu + 33}$	$1 + \frac{2(\cos 2\theta_\nu + 3)}{4\sqrt{2}\sin 2\theta_l \sin^2\theta_\nu - \cos 2\theta_\nu + \cos 2\theta_l(3\cos 2\theta_\nu + 1) - 11}$
J_{CP}	0	$\frac{\sin 2\theta_\nu(\sin 2\theta_l - 2\sqrt{2}\cos 2\theta_l)}{32}$
I_1	0	$\frac{\sin 2\theta_\nu(\cos\theta_l + 3\cos 3\theta_l)(\sqrt{2}\cos\theta_l - 2\sin\theta_l)}{64}$
I_2	0	$-\frac{\sin 2\theta_\nu(\cos\theta_l + 3\cos 3\theta_l)(\sqrt{2}\cos\theta_l - 2\sin\theta_l)}{64}$
(X_l, X_ν, P_l, P_ν)	(U, T, P_{13}, P_{12})	(U, STS, P_{13}, P_{12})
$\sin^2\theta_{13}$	$\frac{(\sin\theta_l(\sqrt{2}\sin\theta_\nu + 2\cos\theta_\nu) + 3\sin\theta_\nu\cos\theta_l)^2}{12}$	$\frac{(2\cos^2\theta_l\cos^2\theta_\nu + \sin^2\theta_\nu(\cos\theta_l + \sqrt{2}\sin\theta_l)^2)}{4}$
$\sin^2\theta_{12}$	$\frac{12(\cos\theta_l - \sqrt{2}\sin\theta_l)^2}{\Delta_2 + 7\cos 2\theta_\nu + 33}$	$-\frac{4(\cos\theta_l - \sqrt{2}\sin\theta_l)^2}{4\sqrt{2}\sin 2\theta_l \sin^2\theta_\nu - \cos 2\theta_\nu + \cos 2\theta_l(3\cos 2\theta_\nu + 1) - 11}$
$\sin^2\theta_{23}$	$1 - \frac{4(\sin\theta_\nu - 2\sqrt{2}\cos\theta_\nu)^2}{\Delta_2 + 7\cos 2\theta_\nu + 33}$	$1 + \frac{2(\cos 2\theta_\nu + 3)}{4\sqrt{2}\sin 2\theta_l \sin^2\theta_\nu - \cos 2\theta_\nu + \cos 2\theta_l(3\cos 2\theta_\nu + 1) - 11}$
J_{CP}	0	$\frac{\sin 2\theta_\nu(2\sqrt{2}\cos 2\theta_l - \sin 2\theta_l)}{32}$
I_1	0	$-\frac{(\cos\theta_l + 3\cos 3\theta_l)\sin 2\theta_\nu(\sqrt{2}\cos\theta_l - 2\sin\theta_l)}{64}$
I_2	0	$\frac{\cos\theta_l\sin 2\theta_\nu(\sqrt{2}(3\cos\theta_l - 7\cos 3\theta_l) + 14\sin\theta_l - 2\sin 3\theta_l)}{64}$
(X_l, X_ν, P_l, P_ν)	(T^2, T, P_{12}, P_{12})	
$\sin^2\theta_{13}$	$\frac{(9\sin^2\theta_\nu\cos^2\theta_l + \sin^2\theta_l(\sqrt{2}\sin\theta_\nu + 2\cos\theta_\nu)^2)}{12}$	
$\sin^2\theta_{12}$	$-\frac{6(\cos 2\theta_l - 3)}{-8\sqrt{2}\sin 2\theta_\nu \sin^2\theta_l + 7\cos 2\theta_\nu + \cos 2\theta_l(11\cos 2\theta_\nu - 3) + 33}$	
$\sin^2\theta_{23}$	$-\frac{4(\sin\theta_\nu - 2\sqrt{2}\cos\theta_\nu)^2}{8\sqrt{2}\sin 2\theta_\nu \sin^2\theta_l + \cos 2\theta_l(3 - 11\cos 2\theta_\nu) - 7\cos 2\theta_\nu - 33}$	
J_{CP}	$-\frac{\sin 2\theta_l(7\sin 2\theta_\nu + 4\sqrt{2}\cos 2\theta_\nu)}{96}$	
I_1	$\frac{(\sin 4\theta_l(12\sqrt{2} - 13\sin 2\theta_\nu) + 14\sin 2\theta_l\sin 2\theta_\nu + 8\sqrt{2}(\sin 2\theta_l + \sin 4\theta_l)\cos 2\theta_\nu)}{192}$	
I_2	$\frac{((14\sin 2\theta_l + 11\sin 4\theta_l)\sin 2\theta_\nu + 32\sqrt{2}\sin^3\theta_l\cos\theta_l\cos 2\theta_\nu)}{192}$	

TABLE III.   Results of the mixing parameters for the independent and viable cases with $(G_l, G_\nu) = (Z_2^{ST^2SU}, Z_2^S)$. Note that the factors $(-1)^{k_1}$ and $(-1)^{k_2}$ are omitted in the expressions of I_1 and I_2 respectively, and they arise from the CP parity matrix $Q_\nu = \mathrm{diag}(1, i^{k_1}, i^{k_2})$.

$(G_l, G_\nu) = (Z_2^{ST^2SU}, Z_2^S)$		
(X_l, X_ν, P_l, P_ν)	$(T^2, 1, P_{12}, P_{13})$	$(T^2, SU, P_{12}, P_{13})$
$\sin^2\theta_{13}$	$\frac{1+\cos 2\theta_l}{4}$	$\frac{1+\cos 2\theta_l}{4}$
$\sin^2\theta_{12}$	$\frac{1}{2}-\frac{\sqrt{2}\sin 2\theta_l \cos(2\theta_\nu+\frac{\pi}{6})}{3-\cos 2\theta_l}$	$\frac{1}{2}+\frac{\sin 2\theta_\nu(1-3\cos 2\theta_l)}{2(3-\cos 2\theta_l)}$
$\sin^2\theta_{23}$	$\frac{2}{3-\cos 2\theta_l}$	$\frac{2}{3-\cos 2\theta_l}$
J_{CP}	$-\frac{\sin 2\theta_l \sin(2\theta_\nu+\frac{\pi}{6})}{8\sqrt{2}}$	$-\frac{\sin 2\theta_l \cos 2\theta_\nu}{8\sqrt{2}}$
I_1	$\frac{(2\sin 2\theta_l-3\sin 4\theta_l)\sin(2\theta_\nu+\frac{\pi}{6})}{16\sqrt{2}}$	$\frac{(3\sin 4\theta_l-2\sin 2\theta_l)\cos 2\theta_\nu}{16\sqrt{2}}$
I_2	$\frac{\cos^2\theta_l(2\sqrt{2}\sin 2\theta_l-\cos(2\theta_\nu+\frac{\pi}{6})(\cos 2\theta_l-3))}{16}$	$-\frac{\sin\theta_l\cos^3\theta_l\cos 2\theta_\nu}{2\sqrt{2}}$
(X_l, X_ν, P_l, P_ν)	$(T^2, TST^2U, P_{12}, P_{13})$	$(U, 1, P_{12}, P_{13})$
$\sin^2\theta_{13}$	$\frac{1+\cos 2\theta_l}{4}$	$\frac{1-\cos 2\theta_l}{4}$
$\sin^2\theta_{12}$	$\frac{(\sqrt{2}\sin\theta_\nu\cos\theta_l-2\sin\theta_l\cos\theta_\nu)^2}{3-\cos 2\theta_l}$	$\frac{1}{2}-\frac{\sqrt{2}\sin 2\theta_l\sin(2\theta_\nu+\frac{\pi}{6})}{3+\cos 2\theta_l}$
$\sin^2\theta_{23}$	$\frac{2}{3-\cos 2\theta_l}$	$\frac{2}{3+\cos 2\theta_l}$
J_{CP}	0	$\frac{\sin 2\theta_l\cos(2\theta_\nu+\frac{\pi}{6})}{8\sqrt{2}}$
I_1	0	$-\frac{(2\sin 2\theta_l+3\sin 4\theta_l)\cos(2\theta_\nu+\frac{\pi}{6})}{16\sqrt{2}}$
I_2	0	$-\frac{\sin^2\theta_l(3\cos 2\theta_l+1)\cos(2\theta_\nu+\frac{\pi}{6})}{16}$
(X_l, X_ν, P_l, P_ν)	$(T^2, 1, P_{13}, P_{13})$	$(T^2, SU, P_{13}, P_{13})$
$\sin^2\theta_{13}$	$\frac{1-\cos 2\theta_l}{4}$	$\frac{1-\cos 2\theta_l}{4}$
$\sin^2\theta_{12}$	$\frac{1}{2}+\frac{\sqrt{2}\sin 2\theta_l\cos(2\theta_\nu+\frac{\pi}{6})}{3+\cos 2\theta_l}$	$\frac{1}{2}+\frac{\sin 2\theta_\nu(1+3\cos 2\theta_l)}{2(3+\cos 2\theta_l)}$
$\sin^2\theta_{23}$	$1-\frac{2}{3+\cos 2\theta_l}$	$1-\frac{2}{3+\cos 2\theta_l}$
J_{CP}	$-\frac{\sin 2\theta_l\sin(2\theta_\nu+\frac{\pi}{6})}{8\sqrt{2}}$	$-\frac{\sin 2\theta_l\cos 2\theta_\nu}{8\sqrt{2}}$
I_1	$-\frac{(2\sin 2\theta_l+3\sin 4\theta_l)\sin(2\theta_\nu+\frac{\pi}{6})}{16\sqrt{2}}$	$\frac{(3\sin 4\theta_l+2\sin 2\theta_l)\cos 2\theta_\nu}{16\sqrt{2}}$
I_2	$\frac{\sin^2\theta_l((\cos 2\theta_l+3)\cos(2\theta_\nu+\frac{\pi}{6})-2\sqrt{2}\sin 2\theta_l)}{16}$	$\frac{\cos\theta_l\sin^3\theta_l\cos 2\theta_\nu}{2\sqrt{2}}$
(X_l, X_ν, P_l, P_ν)	$(T^2, TST^2U, P_{13}, P_{13})$	$(U, 1, P_{13}, P_{13})$
$\sin^2\theta_{13}$	$\frac{1-\cos 2\theta_l}{4}$	$\frac{1+\cos 2\theta_l}{4}$
$\sin^2\theta_{12}$	$\frac{(\sqrt{2}\sin\theta_l\sin\theta_\nu+2\cos\theta_l\cos\theta_\nu)^2}{3+\cos 2\theta_l}$	$\frac{1}{2}+\frac{\sqrt{2}\sin 2\theta_l\sin(2\theta_\nu+\frac{\pi}{6})}{3-\cos 2\theta_l}$
$\sin^2\theta_{23}$	$1-\frac{2}{3+\cos 2\theta_l}$	$1-\frac{2}{3-\cos 2\theta_l}$
J_{CP}	0	$\frac{\sin 2\theta_l\cos(2\theta_\nu+\frac{\pi}{6})}{8\sqrt{2}}$
I_1	0	$\frac{(2\sin 2\theta_l-3\sin 4\theta_l)\cos(2\theta_\nu+\frac{\pi}{6})}{16\sqrt{2}}$
I_2	0	$\frac{\cos^2\theta_l(3\cos 2\theta_l-1)\cos(2\theta_\nu+\frac{\pi}{6})}{16}$
(X_l, X_ν, P_l, P_ν)	$(T^2, TST^2U, P_{13}, P_{12})$	
$\sin^2\theta_{13}$	$\frac{(\sqrt{2}\sin\theta_l\cos\theta_\nu-2\sin\theta_\nu\cos\theta_l)^2}{4}$	
$\sin^2\theta_{12}$	$\frac{4\sin^2\theta_l}{2\sqrt{2}\sin 2\theta_l\sin 2\theta_\nu+\cos 2\theta_\nu+\cos 2\theta_l(3\cos 2\theta_\nu-1)+5}$	
$\sin^2\theta_{23}$	$1-\frac{4\cos^2\theta_\nu}{2\sqrt{2}\sin 2\theta_l\sin 2\theta_\nu+\cos 2\theta_\nu+\cos 2\theta_l(3\cos 2\theta_\nu-1)+5}$	
J_{CP}	0	
I_1	0	
I_2	0	

TABLE IV.   The results of the χ^2 analysis for the independent and viable cases with $(G_l, G_\nu) = (Z_2^{ST^2SU}, Z_2^{TU})$ under the assumption of NH neutrino mass spectrum. χ^2_{min} is the global minimum of χ^2 at the best fitting values $(\theta_l, \theta_\nu)_{bf}$ for θ_l and θ_ν. We give the values of the mixing angles $\sin^2\theta_{13}$, $\sin^2\theta_{12}$, and $\sin^2\theta_{23}$ and the CP-violating phases δ_{CP}, α_{21}, and α_{31} for $(\theta_l, \theta_\nu) = (\theta_l, \theta_\nu)_{bf}$.

(X_l, X_ν, P_l, P_ν)	χ^2_{min}	$(\theta_l, \theta_\nu)_{bf}/\pi$	$\sin^2\theta_{13}$	$\sin^2\theta_{12}$	$\sin^2\theta_{23}$	δ_{CP}/π	α_{21}/π (mod 1)	α_{31}/π (mod 1)
$(U, T, P_{12}, 1)$	0.6354	(0.299, 0.120) (0.093, 0.664)	0.022	0.311	0.437	0	0	0
$(U, T, P_{13}, 1)$	4.6454	(0.803, 0.114) (0.589, 0.669)	0.022	0.317	0.551	1	0	0
(U, T, P_{12}, P_{12})	3.3522	(0.477, 0.072) (0.915, 0.711)	0.022	0.308	0.546	0	0	0
(U, T, P_{13}, P_{12})	0.0010	(0.979, 0.071) (0.413, 0.713)	0.022	0.304	0.451	1	0	0
$(U, STS, P_{12}, 1)$	17.3268	(0.071, 0) (0.071, 1)	0.024	0.344	0.512	0	0	0
$(U, STS, P_{13}, 1)$	16.4425	(0.571, 0) (0.571, 1)	0.024	0.344	0.488	1	0	0
(U, STS, P_{12}, P_{12})	17.3286	(0.929, 0) (0.929, 1)	0.024	0.344	0.512	0	0	0
(U, STS, P_{13}, P_{12})	16.4425	(0.429, 0) (0.429, 1)	0.024	0.344	0.488	1	0	0
(T^2, T, P_{12}, P_{12})	25.7405	(0.075, 0.024) (0.925, 0.024)	0.024	0.270	0.644	1.569	0.728	0.808

Figs. 1, 2, and 3. The most stringent constraint arises from the reactor neutrino mixing angle θ_{13}, which has been measured quite precisely [4–7]. One sees that the three lepton mixing angles θ_{12}, θ_{13}, and θ_{23} can be simultaneously compatible with the experimental data at 3σ level only in a rather narrow region of the $\theta_l - \theta_\nu$ plane. Hence, the mixing angles and CP phases should be able to only vary a bit around the numerical values found in Tables IV,

V, VI, and VII, and consequently the present approach is very predictive. As an example, in Fig. 4, we display the predictions for the CP phases δ_{CP}, α_{21}, and α_{31} in the plane θ_ν vs θ_l for the residual symmetry $(G_l, G_\nu, X_l, X_\nu) = (Z_2^{ST^2SU}, Z_2^S, T^2, SU)$ with $(P_l, P_\nu) = (P_{12}, P_{13})$, (P_{13}, P_{13}), where the small black areas represent the regions in which the experimental data on lepton mixing can be accommodated.

TABLE V.   The results of the χ^2 analysis for the independent and viable cases with $(G_l, G_\nu) = (Z_2^{ST^2SU}, Z_2^{TU})$ under the assumption of the IH neutrino mass spectrum. χ^2_{min} is the global minimum of χ^2 at the best fitting values $(\theta_l, \theta_\nu)_{bf}$ for θ_l and θ_ν. We give the values of the mixing angles $\sin^2\theta_{13}$, $\sin^2\theta_{12}$, and $\sin^2\theta_{23}$ and the CP-violating phases δ_{CP}, α_{21}, and α_{31} for $(\theta_l, \theta_\nu) = (\theta_l, \theta_\nu)_{bf}$.

(X_l, X_ν, P_l, P_ν)	χ^2_{min}	$(\theta_l, \theta_\nu)_{bf}/\pi$	$\sin^2\theta_{13}$	$\sin^2\theta_{12}$	$\sin^2\theta_{23}$	δ_{CP}/π	α_{21}/π (mod 1)	α_{31}/π (mod 1)
$(U, T, P_{12}, 1)$	11.7471	(0.311, 0.140) (0.081, 0.680)	0.023	0.328	0.474	0	0	0
$(U, T, P_{13}, 1)$	0.0011	(0.794, 0.126) (0.597, 0.657)	0.022	0.304	0.580	1	0	0
(U, T, P_{12}, P_{12})	0.6316	(0.480, 0.070) (0.912, 0.714)	0.022	0.302	0.550	0	0	0
(U, T, P_{13}, P_{12})	11.0992	(0.974, 0.075) (0.417, 0.709)	0.022	0.315	0.460	1	0	0
$(U, STS, P_{12}, 1)$	17.6652	(0.071, 0) (0.071, 1)	0.024	0.344	0.512	0	0	0
$(U, STS, P_{13}, 1)$	20.5458	(0.571, 0) (0.571, 1)	0.024	0.344	0.488	1	0	0
(U, STS, P_{12}, P_{12})	17.6652	(0.929, 0) (0.929, 1)	0.024	0.344	0.512	0	0	0
(U, STS, P_{13}, P_{12})	20.5458	(0.429, 0) (0.429, 1)	0.024	0.344	0.488	1	0	0
(T^2, T, P_{12}, P_{12})	17.8338	(0.075, 0.024) (0.925, 0.024)	0.024	0.270	0.644	1.569	0.728	0.808

TABLE VI. The results of the χ^2 analysis for the independent and viable cases with $(G_l, G_\nu) = (Z_2^{ST^2SU}, Z_2^S)$ under the assumption of the NH neutrino mass spectrum. $\chi^2_{\min}$ is the global minimum of χ^2 at the best fitting values $(\theta_l, \theta_\nu)_{\rm bf}$ for θ_l and θ_ν. We give the values of the mixing angles $\sin^2\theta_{13}$, $\sin^2\theta_{12}$, and $\sin^2\theta_{23}$ and the CP-violating phases δ_{CP}, α_{21}, and α_{31} for $(\theta_l, \theta_\nu) = (\theta_l, \theta_\nu)_{\rm bf}$.

(X_l, X_ν, P_l, P_ν)	$\chi^2_{\min}$	$(\theta_l, \theta_\nu)_{\rm bf}/\pi$	$\sin^2\theta_{13}$	$\sin^2\theta_{12}$	$\sin^2\theta_{23}$	δ_{CP}/π	α_{21}/π (mod 1)	α_{31}/π (mod 1)
$(T^2, 1, P_{12}, P_{13})$	17.3286	(0.571, 0.417) (0.429, 0.917)	0.024	0.344	0.512	0	0	0.5
$(T^2, 1, P_{13}, P_{13})$	16.4425	(0.071, 0.417) (0.929, 0.917)	0.024	0.344	0.488	1	0	0.5
$(T^2, SU, P_{12}, P_{13})$	1.2935	(0.433, 0.567) (0.567, 0.933) (0.567, 0.567) (0.433, 0.933)	0.022	0.304	0.511	0.542 1.458	0.208 0.792	0.146 0.854
$(T^2, SU, P_{13}, P_{13})$	0.5023	(0.933, 0.567) (0.067, 0.933) (0.067, 0.567) (0.933, 0.933)	0.022	0.304	0.489	1.542 0.458	0.208 0.792	0.146 0.854
$(T^2, TST^2U, P_{12}, P_{13})$	1.2935	(0.433, 0.266) (0.567, 0.734) (0.433, 0.638) (0.567, 0.362)	0.022	0.304	0.511	0 1	0 0	0 0
$(T^2, TST^2U, P_{13}, P_{13})$	0.5023	(0.933, 0.266) (0.067, 0.734) (0.933, 0.638) (0.067, 0.362)	0.022	0.304	0.489	1 0	0 0	0 0
$(U, 1, P_{12}, P_{13})$	17.3286	(0.071, 0.167) (0.929, 0.667)	0.024	0.344	0.512	0	0	0
$(U, 1, P_{13}, P_{13})$	16.4425	(0.571, 0.167) (0.429, 0.667)	0.024	0.344	0.488	1	0	0
$(T^2, TST^2U, P_{13}, P_{12})$	10.0552	(0.276, 0.165) (0.724, 0.835)	0.022	0.297	0.614	0	0	0

Carefully examining all the numerical results, we see that the predictions for the reactor mixing angel θ_{13} are almost the same while the values of θ_{12}, θ_{23}, and δ_{CP} are considerably different in distinct cases. The current oscillation experiments T2K and NOνA are able to exclude certain ranges of θ_{23} and δ_{CP} around the maximal values, if running in both the neutrino and the antineutrino modes is completed. The forthcoming reactor neutrino oscillation experiments such as JUNO [68] and RENO [69] expect to make a very precise measurement of the solar mixing angle θ_{12}, and the error of $\sin^2\theta_{12}$ can be reduced to about 0.3% [68]. The planned long baseline experiments such as DUNE [70] and Hyper-K [71,72] could significantly improve the precision on θ_{23} and δ_{CP}. Hence, future neutrino facilities have the potential to discriminate among the above possible cases, or rule them out completely.

The neutrinoless double ($0\nu\beta\beta$) decay is a lepton number-violating process. It is an important probe of the Majorana nature of neutrinos, and it can provide us with precious information on the neutrino mass scale and ordering. Searching for $0\nu\beta\beta$ decay has a long history. There are many new sensitive $0\nu\beta\beta$ experiments which are in various stages of planning and construction. The $0\nu\beta\beta$ decay rate is proportional to the effective Majorana mass $|m_{ee}|$ which is expressed in terms of neutrino masses and lepton mixing parameters as [65]

$$
\begin{aligned}
|m_{ee}| &= |m_1 U^2_{\rm PMNS,11} + m_2 U^2_{\rm PMNS,12} + m_3 U^2_{\rm PMNS,13}| \\
&= |m_1\cos^2\theta_{12}\cos^2\theta_{13} + m_2\sin^2\theta_{12}\cos^2\theta_{13}e^{i\alpha_{21}} \\
&\quad + m_3\sin^2\theta_{13}e^{i(\alpha_{31}-2\delta_{CP})}|,
\end{aligned}
\tag{2.91}
$$

where $m_{1,2,3}$ are light neutrino masses. For each admissible case, the allowed regions of the effective Majorana mass $|m_{ee}|$ as a function of the lightest neutrino mass are shown in Figs. 5, 6, and 7. Both parameters θ_1 and θ_2 freely vary between 0 and π, and the three lepton mixing angles are required to lie in their current 3σ ranges [6]. Notice that $|m_{ee}|$ does not depend on θ_{23}. Hence, if two cases have the same residual symmetry but differ in the permutation matrices with $P_l = P_{12}$ and $P_l = P_{13}$ respectively, the same predictions for $|m_{ee}|$ would be obtained. For the case of the IH neutrino mass spectrum, the effective Majorana mass is almost independent of the value of k_2. The reason is because the term in $|m_{ee}|$ proportional to m_3 is suppressed by both $\sin^2\theta_{13}$ and the small value of m_3 itself. Moreover, we see that $|m_{ee}|$ is predicted to be around the upper boundary 0.048 eV, lower boundary 0.015 eV, or

TABLE VII. The results of the χ^2 analysis for the independent and viable cases with $(G_l, G_\nu) = (Z_2^{ST^2SU}, Z_2^S)$ under the assumption of the IH neutrino mass spectrum. χ^2_{min} is the global minimum of χ^2 at the best fitting values $(\theta_l, \theta_\nu)_{bf}$ for θ_l and θ_ν. We give the values of the mixing angles $\sin^2\theta_{13}$, $\sin^2\theta_{12}$, and $\sin^2\theta_{23}$ and the CP-violating phases δ_{CP}, α_{21}, and α_{31} for $(\theta_l, \theta_\nu) = (\theta_l, \theta_\nu)_{bf}$.

(X_l, X_ν, P_l, P_ν)	χ^2_{min}	$(\theta_l, \theta_\nu)_{bf}/\pi$	$\sin^2\theta_{13}$	$\sin^2\theta_{12}$	$\sin^2\theta_{23}$	δ_{CP}/π	α_{21}/π (mod 1)	α_{31}/π (mod 1)
$(T^2, 1, P_{12}, P_{13})$	17.6652	(0.571, 0.417) (0.429, 0.917)	0.024	0.344	0.512	0	0	0.5
$(T^2, 1, P_{13}, P_{13})$	20.5458	(0.071, 0.417) (0.929, 0.917)	0.024	0.344	0.488	1	0	0.5
$(T^2, SU, P_{12}, P_{13})$	3.3575	(0.433, 0.567) (0.567, 0.933) (0.567, 0.567) (0.433, 0.933)	0.022	0.304	0.511	0.542 1.458	0.209 0.791	0.147 0.853
$(T^2, SU, P_{13}, P_{13})$	5.9412	(0.933, 0.567) (0.067, 0.933) (0.067, 0.567) (0.933, 0.933)	0.022	0.304	0.489	1.542 0.458	0.208 0.792	0.146 0.854
$(T^2, TST^2U, P_{12}, P_{13})$	3.3575	(0.433, 0.266) (0.567, 0.734) (0.433, 0.638) (0.567, 0.362)	0.022	0.304	0.511	0 1	0 0	0 0
$(T^2, TST^2U, P_{13}, P_{13})$	5.9412	(0.933, 0.266) (0.067, 0.734) (0.933, 0.638) (0.067, 0.362)	0.022	0.304	0.489	1 0	0 0	0 0
$(U, 1, P_{12}, P_{13})$	17.6652	(0.071, 0.167) (0.929, 0.667)	0.024	0.344	0.512	0	0	0
$(U, 1, P_{13}, P_{13})$	20.5458	(0.571, 0.167) (0.429, 0.667)	0.024	0.344	0.488	1	0	0
$(T^2, TST^2U, P_{13}, P_{12})$	2.2779	(0.276, 0.165) (0.724, 0.835)	0.022	0.297	0.614	0	0	0

close to 0.028 eV for IH. Although these predictions are beyond the reach of the facilities in running, the next generation elaborate $0\nu\beta\beta$ decay experiments are capable of covering the full IH region, such that the present predictions could be tested in near future. For the case of the NH mass spectrum, cancellation between different terms in $|m_{ee}|$ could occur for certain values of the lightest neutrino mass, and consequently the effective mass can be smaller than 10^{-4} eV. However, the range of $m_{lightest}$ in which $|m_{ee}|$ can be quite small is significantly reduced with respect to the generic case. We can even find a nontrivial lower bound on $|m_{ee}|$ in some cases; see e.g. Fig. 5 for the remnant symmetry $(G_l, G_\nu, X_l, X_\nu) = (Z_2^{ST^2SU}, Z_2^{TU}, T^2, T)$ with $P_l = P_\nu = P_{12}$.

III. QUARK FLAVOR MIXING FROM RESIDUAL SYMMETRY $Z_2 \times CP$ IN UP AND DOWN QUARK SECTORS

The Lagrangian for the quark masses and the charged current interactions reads as

$$\mathcal{L} = -\bar{U}_R m_U U_L - \bar{D}_R m_D D_L + \frac{g}{\sqrt{2}}\bar{U}_L \gamma^\mu D_L W_\mu^+ + \text{H.c.},$$

$$(3.1)$$

where $U_R = (u_R, c_R, t_R)^T$, $U_L = (u_L, c_L, t_L)^T$, $D_R = (d_R, s_R, b_R)^T$, and $D_L = (d_L, s_L, b_L)^T$ denote the three left-handed and right-handed up type quark and down type quark fields respectively. It is well known that the mass matrices m_U and m_D can be diagonalized by biunitary transformations,

$$V_u^\dagger m_U U_u = \text{diag}(m_u, m_c, m_t) \equiv \hat{m}_U,$$
$$V_d^\dagger m_D U_d = \text{diag}(m_d, m_s, m_b) \equiv \hat{m}_D. \quad (3.2)$$

The CKM matrix is given by

$$U_{CKM} = U_u^\dagger U_d. \quad (3.3)$$

In this section, we assume that the parent flavor and CP symmetry is broken down to $Z_2^{g_u} \times X_u$ and $Z_2^{g_d} \times X_d$ in the up and down quark sectors respectively, where g_u and g_d denote the generators of the Z_2 residual flavor symmetry groups with $g_u^2 = g_d^2 = 1$. Similarly to the lepton sector, we assign the three generations of left-handed quarks to a three-dimensional representation **3**. The mass matrices m_U and m_D respect the residual symmetries $Z_2^{g_u} \times X_u$ and $Z_2^{g_d} \times X_d$ respectively, and they should fulfill
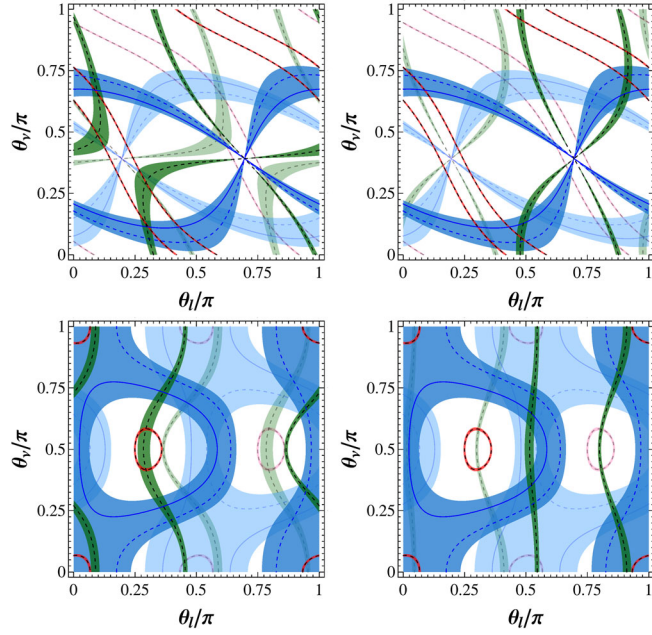
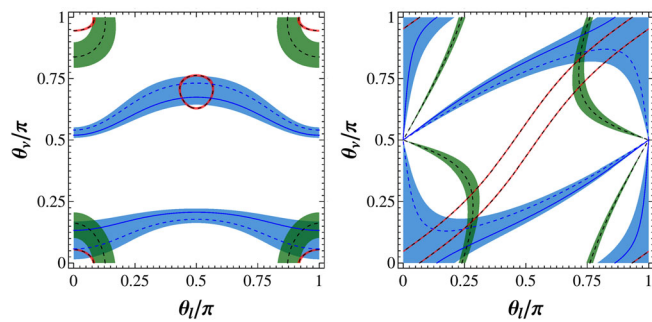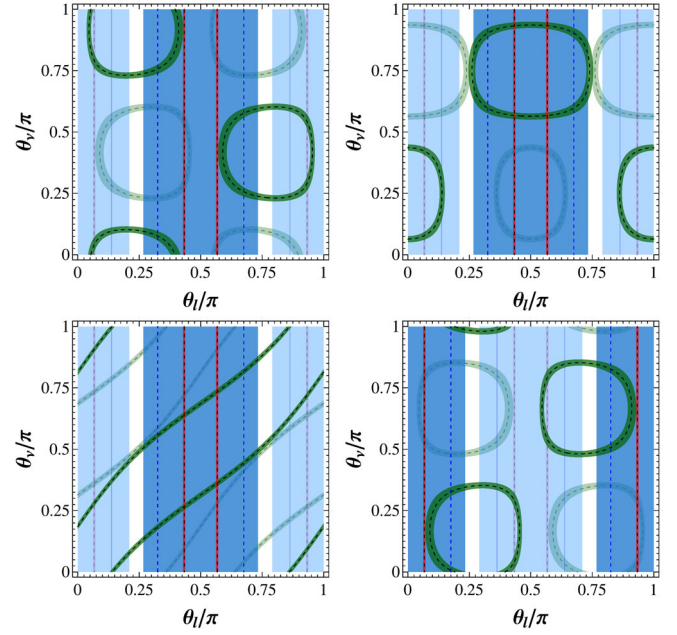FIG. 1. The contour plots of $\sin^2 \theta_{ij}$ in the plane θ_ν vs θ_l. The red, blue, and green areas denote the 3σ regions of $\sin^2 \theta_{13}$, $\sin^2 \theta_{23}$, and $\sin^2 \theta_{12}$ respectively. The dashed (or solid) lines indicate the best fit values of the mixing angles. Notice that the best fit value of $\sin^2 \theta_{23}$ depends on the neutrino mass ordering, and the solid and dashed lines are for NH and IH respectively. The residual flavor symmetry is $(G_l, G_\nu) = (Z_2^{ST^2SU}, Z_2^{TU})$ in this case. The first row corresponds to $(X_l, X_\nu, P_l, P_\nu) = (U, T, P_{12}, 1)$ on the left panel and $(X_l, X_\nu, P_l, P_\nu) = (U, T, P_{12}, P_{12})$ on the right panel, and the last row is for $(X_l, X_\nu, P_l, P_\nu) = (U, STS, P_{12}, 1)$, (U, STS, P_{12}, P_{12}). The foreground and background differ in the values of P_l which are equal to P_{12} and P_{13} respectively.

FIG. 3. The contour plots of $\sin^2 \theta_{ij}$ in the plane θ_ν vs θ_l. The red, blue, and green areas denote the 3σ regions of $\sin^2 \theta_{13}$, $\sin^2 \theta_{23}$, and $\sin^2 \theta_{12}$ respectively. The dashed (or solid) lines indicate the best fit values of the mixing angles. Notice that the best fit value of $\sin^2 \theta_{23}$ depends on the neutrino mass ordering, and the solid and dashed lines are for NH and IH respectively. The residual flavor symmetry is $(G_l, G_\nu) = (Z_2^{ST^2SU}, Z_2^S)$ in this case. The first row corresponds to $(X_l, X_\nu, P_l, P_\nu) = (T^2, 1, P_{12}, P_{13})$ on the left panel and $(X_l, X_\nu, P_l, P_\nu) = (T^2, SU, P_{12}, P_{13})$ on the right panel, and the last row is for $(X_l, X_\nu, P_l, P_\nu) = (T^2, TST^2U, P_{13}, P_{13})$, $(U, 1, P_{12}, P_{13})$. The foreground and background differ in the values of P_l which are equal to P_{12} and P_{13} respectively.

FIG. 2. The contour plots of $\sin^2 \theta_{ij}$ in the plane θ_ν vs θ_l. The red, blue, and green areas denote the 3σ regions of $\sin^2 \theta_{13}$, $\sin^2 \theta_{23}$, and $\sin^2 \theta_{12}$ respectively. The dashed (or solid) lines indicate the best fit values of the mixing angles. Notice that the best fit value of $\sin^2 \theta_{23}$ depends on the neutrino mass ordering, and the solid and dashed lines are for NH and IH respectively. The left and right panels correspond to $(G_l, G_\nu, X_l, X_\nu, P_l, P_\nu) = (Z_2^{ST^2SU}, Z_2^{TU}, T^2, T, P_{12}, P_{12})$ and $(Z_2^{ST^2SU}, Z_2^S, T^2, TST^2U, P_{13}, P_{12})$ respectively.

$$\rho_3^\dagger(g_u)m_U^\dagger m_U \rho_3(g_u) = m_U^\dagger m_U, \quad X_u^\dagger m_U^\dagger m_U X_u = (m_U^\dagger m_U)^*,$$
$$\rho_3^\dagger(g_d)m_D^\dagger m_D \rho_3(g_d) = m_D^\dagger m_D, \quad X_d^\dagger m_D^\dagger m_D X_d = (m_D^\dagger m_D)^*. \tag{3.4}$$

Following the procedures presented in Sec. II A, the constraints on the unitary transformations U_u and U_d from the postulated residual symmetries can be straightforwardly extracted. A critical step is the Takagi factorization of the residual CP transformations X_u and X_d which have the following properties:

$$X_u = \Sigma_u \Sigma_u^T, \qquad \Sigma_u^\dagger \rho_3(g_u)\Sigma_u = \mathrm{diag}(1, -1, -1), \tag{3.5}$$

$$X_d = \Sigma_d \Sigma_d^T, \qquad \Sigma_d^\dagger \rho_3(g_d)\Sigma_d = \mathrm{diag}(1, -1, -1). \tag{3.6}$$

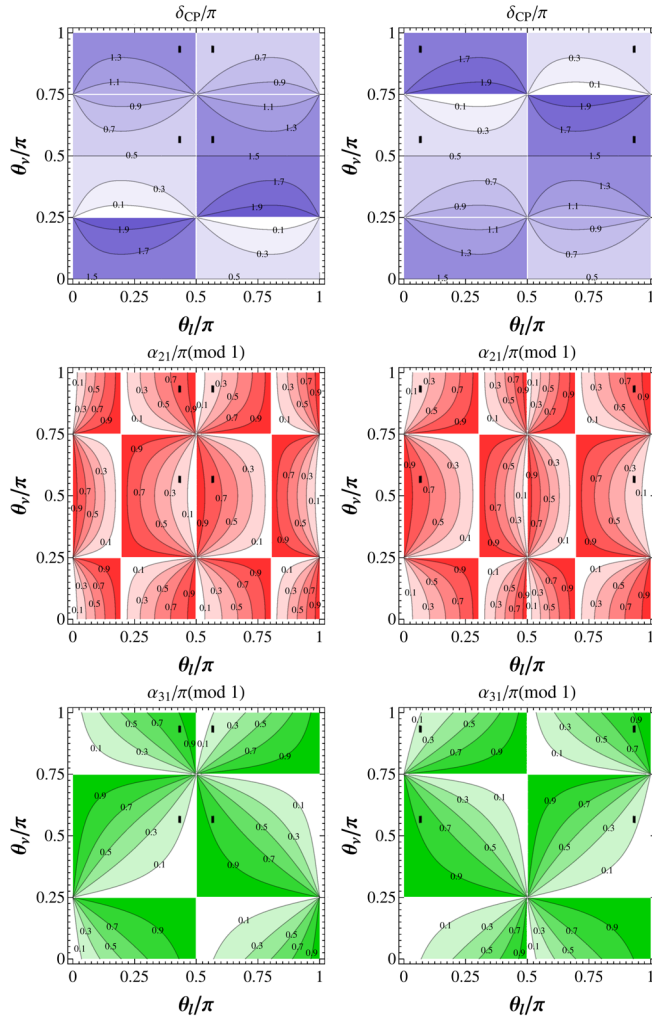Then following the same procedure of deriving Eq. (2.51), we can obtain the CKM mixing matrix is of the form

FIG. 4. The contour plots of the *CP*-violation phases δ_{CP}, α_{21}, and α_{31} in the plane θ_ν vs θ_l. The black areas denote the regions in which the lepton mixing angles are compatible with experimental data at 3σ level. The residual symmetry is $(G_l, G_\nu, X_l, X_\nu) = (Z_2^{ST^2SU}, Z_2^S, T^2, SU)$. The figures on the right-hand and left-hand sides correspond to the row and column permutations $(P_l, P_\nu) = (P_{12}, P_{13})$ and $(P_l, P_\nu) = (P_{13}, P_{13})$ respectively.

$$U_{\text{CKM}} = Q_u P_u S_{23}(\theta_u) \Sigma_u^\dagger \Sigma_d S_{23}(\theta_d) P_d Q_d, \quad (3.7)$$

where Q_u and Q_d are generic diagonal matrices of phases, they can be removed by utilizing the rephasing freedom of the up and down quarks, and P_u and P_d are permutation matrices. Similarly to the master formula of the lepton flavor mixing in Eq. (2.51), the CKM mixing matrix is determined up to possible permutations of rows and columns, and it depends on two free parameters θ_u and θ_d which can take values between 0 and π.

In the same fashion as Sec. II B, we can find the condition under which the CKM matrices predicted by two distinct residual symmetries are equivalent. We generically denote the combination $U_q \equiv \Sigma_u^\dagger \Sigma_d$ for any two postulated residual symmetries as

$$U_q = \begin{pmatrix} a_1 & a_2 & a_3 \\ a_4 & a_5 & a_6 \\ a_7 & a_8 & a_9 \end{pmatrix},$$

$$U_q' = \begin{pmatrix} b_1 & b_2 & b_3 \\ b_4 & b_5 & b_6 \\ b_7 & b_8 & b_9 \end{pmatrix}, \quad (3.8)$$

where a_1 and b_1 are fixed by remnant symmetries up to an overall phase. The corresponding CKM mixing matrices cannot be effectively the same one if $|a_1| \neq |b_1|$. In the following, we shall focus on the case of $a_1 = b_1 = 0$. The results for the most general case $|a_1| = |b_1| \neq 0$, 1 are summarized in Appendix B. After some straightforward algebra, the conditions of equivalence can be described as follows:

(i) $b_2^2 + b_3^2 \neq 0$, $b_4^2 + b_7^2 \neq 0$:

The assumed remnant symmetries would lead to the same quark mixing pattern if the following equalities are satisfied,

$$|a_2^2 + a_3^2| = |b_2^2 + b_3^2|,$$
$$(a_2 b_2 + a_3 b_3)(a_2^* b_3^* - a_3^* b_2^*) \in \mathbb{R},$$
$$|a_4^2 + a_7^2| = |b_4^2 + b_7^2|,$$
$$(a_4 b_4 + a_7 b_7)(a_4^* b_7^* - a_7^* b_4^*) \in \mathbb{R},$$
$$t_i T_j - t_j T_i = 0,$$
$$|t_i| = |T_i|,$$
$$i, j = 5, 6, 8, 9, \quad (3.9)$$

where

$$t_5 = (xb_5 + yb_6)z + (xb_8 + yb_9)w,$$
$$t_6 = (xb_6 - yb_5)z + (xb_9 - yb_8)w,$$
$$t_8 = (xb_8 + yb_9)z - (xb_5 + yb_6)w,$$
$$t_9 = (xb_9 - yb_8)z - (xb_6 - yb_5)w, \quad (3.10)$$

and

$$T_5 = (b_2^2 + b_3^2)(b_4^2 + b_7^2)a_5,$$
$$T_6 = (b_2^2 + b_3^2)(b_4^2 + b_7^2)a_6,$$
$$T_8 = (b_2^2 + b_3^2)(b_4^2 + b_7^2)a_8,$$
$$T_9 = (b_2^2 + b_3^2)(b_4^2 + b_7^2)a_9, \quad (3.11)$$

with

$$x = a_2 b_2 + a_3 b_3, \qquad y = a_2 b_3 - a_3 b_2,$$
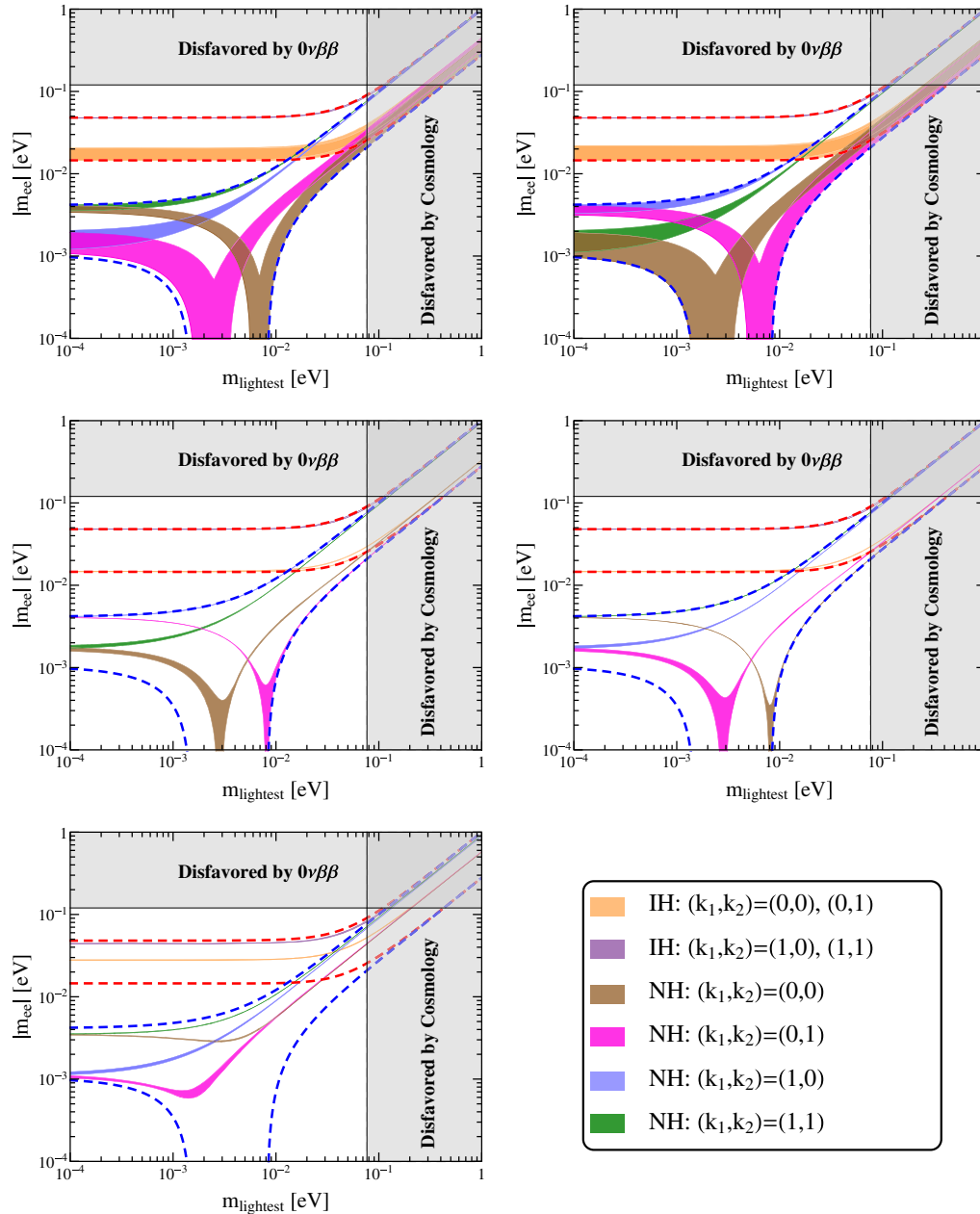$$z = a_4 b_4 + a_7 b_7, \qquad w = a_4 b_7 - a_7 b_4. \quad (3.12)$$

FIG. 5.   The predictions for the possible values of the effective Majorana mass $|m_{ee}|$ as a function of the lightest neutrino mass. The red (blue) dashed lines indicate the most general allowed regions for the IH (NH) neutrino mass spectrum obtained by varying the mixing parameters over the 3σ ranges [6]. The residual flavor symmetry is $(G_l, G_\nu) = (Z_2^{ST^2SU}, Z_2^{TU})$ in this case. The first row corresponds to $(X_l, X_\nu, P_l, P_\nu) = (U, T, P_{12}, 1)$ on the left and $(X_l, X_\nu, P_l, P_\nu) = (U, T, P_{12}, P_{12})$ on the right, the middle row is for $(X_l, X_\nu, P_l, P_\nu) = (U, STS, P_{12}, 1)$, (U, STS, P_{12}, P_{12}), and the last row is for $(X_l, X_\nu, P_l, P_\nu) = (T^2, T, P_{12}, P_{12})$. The present most stringent upper limits $|m_{ee}| < 0.120$ eV from EXO-200 [73,74] and KamLAND-ZEN [75] are shown by a horizontal gray band. The vertical gray exclusion band is the current limit on the lightest neutrino masses from the cosmological data $\sum m_i < 0.230$ eV at 95% confidence level obtained by the Planck Collaboration [76].
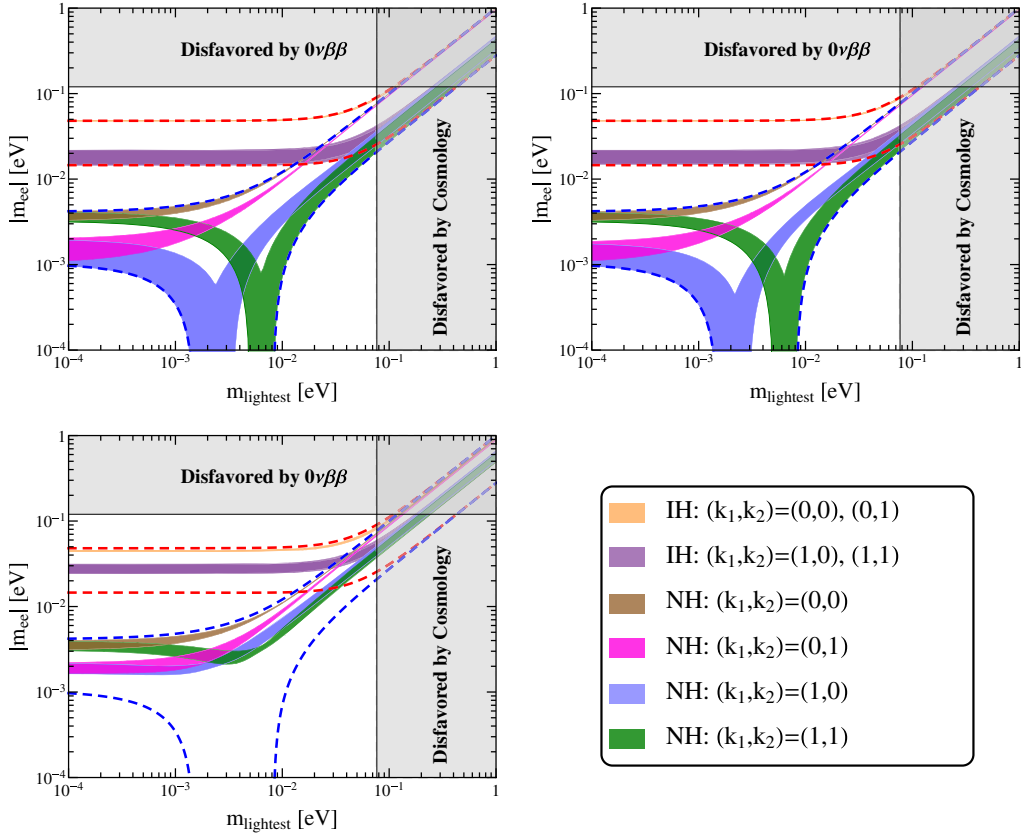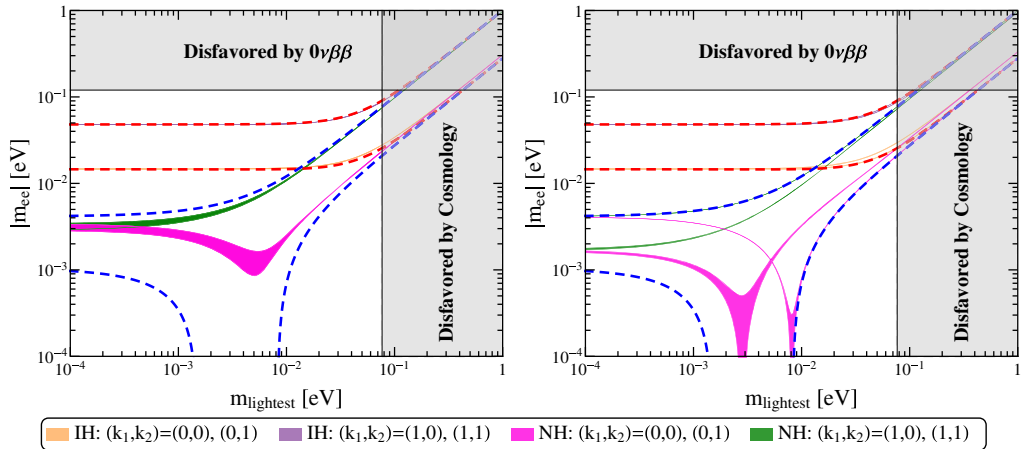
FIG. 6. The predictions for the effective Majorana mass $|m_{ee}|$, where we use the same conventions as in Fig. 5. The residual flavor symmetry is $(G_l, G_\nu) = (Z_2^{ST^2SU}, Z_2^S)$ in this case. The top left panel corresponds to $(X_l, X_\nu, P_l, P_\nu) = (T^2, TST^2U, P_{12}, P_{13})$, the top right panel is for $(X_l, X_\nu, P_l, P_\nu) = (T^2, TST^2U, P_{13}, P_{12})$, and the last one is for $(X_l, X_\nu, P_l, P_\nu) = (T^2, SU, P_{12}, P_{13})$.

FIG. 7. The predictions for the effective Majorana mass $|m_{ee}|$, where we use the same conventions as in Fig. 5. The residual flavor symmetry is $(G_l, G_\nu) = (Z_2^{ST^2SU}, Z_2^S)$ in this case. The panels on the right-hand and left-hand sides correspond to $(X_l, X_\nu, P_l, P_\nu) = (T^2, 1, P_{12}, P_{13})$ and $(X_l, X_\nu, P_l, P_\nu) = (U, 1, P_{12}, P_{13})$ respectively. Notice that $|m_{ee}|$ is invariant under the transformations $\theta_l \to \pi - \theta_l$, $\theta_\nu \to \theta_\nu + \pi/2$ and $k_2 \to k_2 + 1$, and hence the effective mass is independent of k_2 in this case.

(ii) $b_2^2 + b_3^2 = 0$, $b_4^2 + b_7^2 \neq 0$:

The necessary and sufficient conditions for the equivalence of these two CKM matrices are found to be

$$|a_4^2 + a_7^2| = |b_4^2 + b_7^2|,$$

$$(a_4 b_4 + a_7 b_7)(a_4^* b_7^* - a_7^* b_4^*) \in \mathbb{R},$$

$$a_2 b_2 + a_3 b_3 = 0,$$

$$t_5 T_8 - t_8 T_5 = 0,$$

$$|t_5| = |T_5|,$$

$$|t_8| = |T_8|, \qquad (3.13)$$

with

$$t_5 = (zb_5 + wb_8)a_2^*, \qquad t_8 = (zb_8 - wb_5)a_2^*,$$

$$T_5 = (b_4^2 + b_7^2)b_2^* a_5, \qquad T_8 = (b_4^2 + b_7^2)b_2^* a_8.$$

$$(3.14)$$

(iii) $b_2^2 + b_3^2 \neq 0$, $b_4^2 + b_7^2 = 0$:

In this case, the equivalence condition is given by

$$|a_2^2 + a_3^2| = |b_2^2 + b_3^2|,$$

$$(a_2 b_2 + a_3 b_3)(a_2^* b_3^* - a_3^* b_2^*) \in \mathbb{R},$$

$$a_4 b_4 + a_7 b_7 = 0,$$

$$t_5 T_6 - t_6 T_5 = 0,$$

$$|t_5| = |T_5|,$$

$$|t_6| = |T_6|, \qquad (3.15)$$

where

$$t_5 = (xb_5 + yb_6)a_4^*, \qquad t_6 = (xb_6 - yb_5)a_4^*,$$

$$T_5 = (b_2^2 + b_3^2)b_4^* a_5, \qquad T_6 = (b_2^2 + b_3^2)b_4^* a_6.$$

$$(3.16)$$

(iv) $b_2^2 + b_3^2 = 0$, $b_4^2 + b_7^2 = 0$:

After the freedom to redefine the free parameters θ_u and θ_d is taken into account, the same quark mixing pattern would be obtained if the parameters a_i and b_i are subject to the following constraints:

$$a_2 b_2 + a_3 b_3 = 0, \qquad a_4 b_4 + a_7 b_7 = 0. \qquad (3.17)$$

Notice that if the conditions of any of the above four cases are satisfied under the substitutions

$$a_1 \rightarrow a_1, \qquad a_2 \rightarrow a_2, \qquad a_3 \rightarrow s_2 a_2,$$

$$a_4 \rightarrow a_4, \qquad a_5 \rightarrow a_5, \qquad a_6 \rightarrow s_2 a_6,$$

$$a_7 \rightarrow s_1 a_7, \qquad a_8 \rightarrow s_1 a_8, \qquad a_9 \rightarrow s_1 s_2 a_9,$$

$$(3.18)$$

with $s_{1,2} = \pm 1$, the assumed remnant symmetries would give rise to the same quark mixing.

So far, the CKM mixing matrix has been measured quite accurately. The present global fit result for the magnitude of each CKM matrix element is [77]

$$|U_{\text{CKM}}| = \begin{pmatrix} 0.97431 \pm 0.00015 & 0.22512 \pm 0.00067 & 0.00365 \pm 0.00012 \\ 0.22497 \pm 0.00067 & 0.97344 \pm 0.00015 & 0.04255 \pm 0.00069 \\ 0.00869 \pm 0.00014 & 0.04156 \pm 0.00056 & 0.999097 \pm 0.000024 \end{pmatrix}. \qquad (3.19)$$

The full fit values of three quark mixing angles read as [77]

$$\sin\theta_{12}^q = 0.22497 \pm 0.00069, \quad \sin\theta_{23}^q = 0.04229 \pm 0.00057,$$

$$\sin\theta_{13}^q = 0.00368 \pm 0.00010. \qquad (3.20)$$

Now, let us concentrate on the S_4 flavor symmetry group as an illustrative example. Considering all the possible residual subgroups $Z_2 \times CP$ arising from the original S_4 and CP symmetry, we find the fixed element can be 0, 1/2, $1/\sqrt{2}$, or 1. According to experimental data shown in Eq. (3.19), a vanishing (13) or (31) element of the CKM matrix is a good leading order approximation, since the (13) and (31) entries are very small and this tiny discrepancy could be easily resolved in an explicit model with small corrections. All three quark mixing angles except θ_{13}^q can be accommodated very well for the representative remnant symmetries $G_u = Z_2^{ST^2SU} \times T^2$ and $G_d = Z_2^{T^2U} \times T^2$ in the up and down quark sectors respectively. The corresponding Takagi factorization matrices Σ_u and Σ_d are determined to be

$$\Sigma_u = \frac{1}{\sqrt{6}} \begin{pmatrix} 2 & 0 & -\sqrt{2} \\ e^{i\pi/3} & -\sqrt{3}e^{i\pi/3} & \sqrt{2}e^{i\pi/3} \\ e^{-i\pi/3} & \sqrt{3}e^{-i\pi/3} & \sqrt{2}e^{-i\pi/3} \end{pmatrix},$$

$$\Sigma_d = \frac{1}{\sqrt{2}} \begin{pmatrix} 0 & 0 & \sqrt{2} \\ -e^{i\pi/3} & e^{i\pi/3} & 0 \\ e^{-i\pi/3} & e^{-i\pi/3} & 0 \end{pmatrix}. \qquad (3.21)$$

For the permutation matrices $P_u = 1$ and $P_d = P_{13}$, we find $U_{\text{CKM}}(1,3) = 0$, and the CKM matrix takes the form

$$U_{\text{CKM}} = \frac{1}{\sqrt{3}} \begin{pmatrix} \sqrt{2}\cos\theta_d + \sin\theta_d & \cos\theta_d - \sqrt{2}\sin\theta_d & 0 \\ (\sqrt{2}\sin\theta_d - \cos\theta_d)\sin\theta_u & (\sqrt{2}\cos\theta_d + \sin\theta_d)\sin\theta_u & \sqrt{3}\cos\theta_u \\ (\sqrt{2}\sin\theta_d - \cos\theta_d)\cos\theta_u & (\sqrt{2}\cos\theta_d + \sin\theta_d)\cos\theta_u & -\sqrt{3}\sin\theta_u \end{pmatrix}, \qquad (3.22)$$

from which we can extract the quark mixing angles as

$$\sin^2\theta_{13}^q = 0, \qquad \sin^2\theta_{12}^q = \frac{1}{3}(\cos\theta_d - \sqrt{2}\sin\theta_d)^2, \qquad \sin^2\theta_{23}^q = \cos^2\theta_u. \qquad (3.23)$$

The best fitting values of θ_{12}^q and θ_{23}^q in Eq. (3.20) can be obtained for

$$(\theta_u, \theta_d) = (0.513\pi, 0.124\pi), \qquad (0.513\pi, 0.268\pi), \qquad (0.487\pi, 0.124\pi), \qquad (0.487\pi, 0.268\pi). \qquad (3.24)$$

We expect that the small mixing angle θ_{13}^q as well as the CP-violation phase can be generated by higher order contributions in a concrete model. For the values $P_u = P_{13}$ and $P_d = 1$, we have $U_{\text{CKM}}(3,1) = 0$. The CKM mixing matrix is given by

$$U_{\text{CKM}} = \frac{1}{\sqrt{3}} \begin{pmatrix} -\sqrt{3}\sin\theta_u & (\sqrt{2}\cos\theta_d + \sin\theta_d)\cos\theta_u & (\sqrt{2}\sin\theta_d - \cos\theta_d)\cos\theta_u \\ \sqrt{3}\cos\theta_u & (\sqrt{2}\cos\theta_d + \sin\theta_d)\sin\theta_u & (\sqrt{2}\sin\theta_d - \cos\theta_d)\sin\theta_u \\ 0 & \cos\theta_d - \sqrt{2}\sin\theta_d & \sqrt{2}\cos\theta_d + \sin\theta_d \end{pmatrix}. \qquad (3.25)$$

The mixing angles read

$$\sin^2\theta_{13}^q = \frac{1}{3}\cos^2\theta_u(\cos\theta_d - \sqrt{2}\sin\theta_d)^2,$$

$$\sin^2\theta_{12}^q = \frac{4\cos^2\theta_u(\sin\theta_d + \sqrt{2}\cos\theta_d)^2}{9 - 3\cos 2\theta_u + 2\cos^2\theta_u(2\sqrt{2}\sin 2\theta_d + \cos 2\theta_d)},$$

$$\sin^2\theta_{23}^q = \frac{4\sin^2\theta_u(\cos\theta_d - \sqrt{2}\sin\theta_d)^2}{9 - 3\cos 2\theta_u + 2\cos^2\theta_u(2\sqrt{2}\sin 2\theta_d + \cos 2\theta_d)}. \qquad (3.26)$$

In this case, the central values of θ_{12}^q and θ_{23}^q can be obtained for

$$(\theta_u, \theta_d) = (0.428\pi, 0.182\pi), \qquad (0.428\pi, 0.210\pi),$$
$$(0.572\pi, 0.182\pi), \qquad (0.572\pi, 0.210\pi). \qquad (3.27)$$

We display the contour plot of $\sin\theta_{13}^q$, $\sin\theta_{12}^q$, and $\sin\theta_{23}^q$ in the plane θ_d vs θ_u in Fig. 8. If the best fit values of θ_{12}^q and θ_{23}^q are reproduced, we see that $\sin\theta_{13}^q$ would be approximately three times as large as its measured value. However, accordance with the experimental data could be easily achieved in a concrete model after subleading corrections are taken into account.

IV. LEPTON FLAVOR MIXING FROM SINGLE RESIDUAL CP TRANSFORMATION IN THE NEUTRINO SECTOR

In this section, we shall instead consider the scenario in which the residual symmetry of the charged lepton sector is an Abelian subgroup and the neutrino mass matrix m_ν is
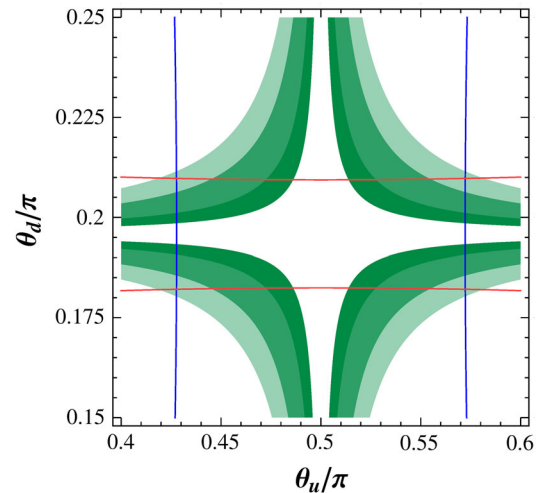

FIG. 8. The contour plot of $\sin\theta_{13}^q$, $\sin\theta_{12}^q$, and $\sin\theta_{23}^q$ in the $\theta_d - \theta_u$ plane. The blue and red lines denote the central values of $\sin\theta_{12}^q$ and $\sin\theta_{23}^q$ respectively. The different shading areas from dark green to light green represent three interesting regions of $\sin\theta_{13}^q$ such as $0.5(\sin\theta_{13}^q)_{\text{bf}} \to (\sin\theta_{13}^q)_{\text{bf}}$, $(\sin\theta_{13}^q)_{\text{bf}} \to 2(\sin\theta_{13}^q)_{\text{bf}}$, and $2(\sin\theta_{13}^q)_{\text{bf}} \to 3(\sin\theta_{13}^q)_{\text{bf}}$, where we use $(\sin\theta_{13}^q)_{\text{bf}} = 0.00368$.

invariant under a single residual CP transformation X_ν. In order to avoid partially degenerate neutrino masses, X_ν should be a symmetric unitary matrix with $X_\nu = X_\nu^T$ and $X_\nu X_\nu^* = 1$ [24,27–29]. As a result, m_ν is invariant under the action of X_ν,

$$X_\nu^T m_\nu X_\nu = m_\nu^*. \tag{4.1}$$

Without reconstructing the neutrino mass matrix, from this equation, we can derive that the unitary transformation U_ν, which is the a diagonalization matrix of m_ν with $U_\nu^T m_\nu U_\nu = \mathrm{diag}(m_1, m_2, m_3)$, is subject to the following constraint [27,29],

$$U_\nu^\dagger X_\nu U_\nu^* = \mathrm{diag}(\pm 1, \pm 1, \pm 1) \equiv Q_\nu^2, \tag{4.2}$$

where Q_ν is a diagonal matrix with nonvanishing entries ± 1 and $\pm i$ to make the light neutrino masses positive definite, and it can be parametrized as Eq. (2.31). Performing Takagi factorization $X_\nu = \Sigma_\nu \Sigma_\nu^T$ where Σ_ν is unitary, we obtain

$$(\Sigma_\nu^T U_\nu^* Q_\nu)^T (\Sigma_\nu^T U_\nu^* Q_\nu) = 1. \tag{4.3}$$

Therefore, $\Sigma_\nu^T U_\nu^* Q_\nu$ is a real orthogonal matrix

$$\Sigma_\nu^T U_\nu^* Q_\nu = O_{3\times 3}, \tag{4.4}$$

where $O_{3\times 3}$ can be parametrized as

$$O_{3\times 3} = \begin{pmatrix} 1 & 0 & 0 \\ 0 & \cos\theta_1 & \sin\theta_1 \\ 0 & -\sin\theta_1 & \cos\theta_1 \end{pmatrix} \begin{pmatrix} \cos\theta_2 & 0 & \sin\theta_2 \\ 0 & 1 & 0 \\ -\sin\theta_2 & 0 & \cos\theta_2 \end{pmatrix}$$
$$\times \begin{pmatrix} \cos\theta_3 & \sin\theta_3 & 0 \\ -\sin\theta_3 & \cos\theta_3 & 0 \\ 0 & 0 & 1 \end{pmatrix},$$

where the fundamental interval of the real parameters $\theta_{1,2,3}$ is $[0, \pi)$. Thus, the neutrino mixing matrix is determined to be of the form [25,26]

$$U_\nu = \Sigma_\nu O_{3\times 3} Q_\nu. \tag{4.5}$$

The flavor symmetry is assumed to be broken to an Abelian subgroup G_l in the charged lepton sector, and the generator of G_l is denoted as g_l.[1] The charged lepton mass matrix m_l would fulfill

$$\rho_{\mathbf{3}}^\dagger(g_l) m_l^\dagger m_l \rho_{\mathbf{3}}(g_l) = m_l^\dagger m_l. \tag{4.6}$$

---

[1] Here, we assume G_l is generated by a single generator, and the generalization to the case in which G_l has several generators is straightforward.

Thus, we find that the unitary transformation U_l which diagonalizes $m_l^\dagger m_l$ is constrained to satisfy

$$U_l^\dagger \rho_{\mathbf{3}}(g_l) U_l = \rho_{\mathbf{3}}^{\mathrm{diag}}(g_l), \tag{4.7}$$

where $\rho_{\mathbf{3}}^{\mathrm{diag}}(g_l)$ is a diagonal phase matrix. That is to say, the charged lepton mixing matrix U_l can be obtained by diagonalizing the representation matrix of the generator g_l without resorting to the mass matrix. Here, we assume that the residual symmetry G_l can distinguish among the three charged leptons, and consequently U_l is uniquely determined up to permutations and phases of its column vectors. As a result, the PMNS mixing matrix is found to be of the form

$$U_{\mathrm{PMNS}} = Q_l P_l U_l^\dagger \Sigma_\nu O_{3\times 3} Q_\nu, \tag{4.8}$$

where P_l is an arbitrary three-dimensional permutation matrix, Q_l is a diagonal unitary matrix which can be absorbed into the charged lepton fields. If two pairs of residual subgroups $\{G_l, X_\nu\}$ and $\{G_l', X_\nu'\}$ are related by a similarity transformation Ω,

$$\rho_{\mathbf{3}}(g_l') = \Omega \rho_{\mathbf{3}}(g_l) \Omega^\dagger, \quad X_\nu' = \Omega X_\nu \Omega^T, \tag{4.9}$$

both pairs would lead to the same result for U_{PMNS}. The reason is because the Takagi factorization of X_ν' is $\Omega \Sigma_\nu$ and $\rho_{\mathbf{3}}(g_l')$ is diagonalized by ΩU_l.

A. Condition for the equivalence of two mixing patterns

Let us assume two different residual symmetries $\{G_l, X_\nu\}$ and $\{G_l', X_\nu'\}$; accordingly, the PMNS matrices are predicted to be

$$U_{\mathrm{PMNS}} = Q_l P_l U_l^\dagger \Sigma_\nu O_{3\times 3} Q_\nu, \tag{4.10}$$

$$U'_{\mathrm{PMNS}} = Q_l' P_l' U_l'^\dagger \Sigma_\nu' O_{3\times 3}' Q_\nu'. \tag{4.11}$$

For any given value of the real orthogonal matrix $O_{3\times 3}$, if one can always find a corresponding orthogonal matrix $O_{3\times 3}'$ as well as Q_l', P_l', and Q_ν', such that the equality

$$U_{\mathrm{PMNS}} = U'_{\mathrm{PMNS}} \tag{4.12}$$

is fulfilled, then these two mixing patterns would be essentially the same. From Eq. (4.12), we can obtain the condition

$$U O_{3\times 3} = Q_L P_L U' O_{3\times 3}' Q_N, \tag{4.13}$$

with

$$U \equiv U_l^\dagger \Sigma_\nu, \qquad U' \equiv U_l'^\dagger \Sigma_\nu', \qquad P_L \equiv P_l^T P_l',$$

$$Q_L \equiv P_l^T Q_l^\dagger Q_l' P_l, \qquad Q_N \equiv Q_\nu' Q_\nu^\dagger. \qquad (4.14)$$

Both sides of Eq. (4.13) multiply with their transpose, and we have

$$UU^T = Q_L P_L U' O'_{3\times 3} Q_N^2 O'^T_{3\times 3} U'^T P_L^T Q_L. \qquad (4.15)$$

Notice that Q_N is a diagonal matrix with entries ± 1 and $\pm i$, and Eq. (4.15) is satisfied for a generic orthogonal matrix $O'_{3\times 3}$. This requires $Q_N^2 = \pm \mathrm{diag}(1,1,1)$, and Q_N^2 can be set to be an identity matrix by choosing suitable values of Q_ν and Q'_ν. Thus, the condition for the equivalence of the two mixing patterns in this scenario simplifies into

$$UU^T = Q_L P_L U' U'^T P_L^T Q_L. \qquad (4.16)$$

Inversely, if we can find a permutation matrix P_L and a phase matrix Q_L such that Eq. (4.16) is fulfilled, the postulated residual symmetries would lead to the same lepton mixing pattern.

B. Examples in S_4 and CP

In this section, we shall analyze the lepton mixing patterns which arise from the breaking of the flavor group S_4 and CP symmetry to an Abelian subgroup G_l in the charged lepton sector and to a residual CP X_ν in the neutrino sector. We shall consider all possibilities for G_l, i.e., $G_l = Z_3, Z_4, K_4$, and all possible residual CP transformation X_ν which should be a unitary symmetric matrix,

$$X_\nu = \{1, S, T, T^2, STS, ST^2S, U, SU, TST^2U, T^2STU\}, \qquad (4.17)$$

where we do not distinguish between the abstract elements of the S_4 group and their representation matrices in **3** for simplicity of notation. In fact, it is not necessary to study the mixing patterns comprehensively for all possible combinations of G_l and X_ν. By applying the general equivalence criterion in Eq. (4.16), we find there are only five independent cases with $(G_l, X_\nu) = (Z_3^T, 1)$, (Z_3^T, S), (Z_3^T, U), (Z_3^T, SU), and $(K_4^{(S,U)}, T)$. In the following, we take into account all possible row permutations of the mixing matrix in each case, and the predictions for lepton mixing angles and CP-violation phases as well as neutrinoless double decay will be investigated:

  (i) $G_l = Z_3^T, X_\nu = 1$:

    In this case, the unitary matrices U_l and Σ_ν are given by

$$U_l = \begin{pmatrix} 1 & 0 & 0 \\ 0 & 1 & 0 \\ 0 & 0 & 1 \end{pmatrix}, \quad \Sigma_\nu = \begin{pmatrix} 1 & 0 & 0 \\ 0 & 1 & 0 \\ 0 & 0 & 1 \end{pmatrix}. \qquad (4.18)$$

Moreover, we find that the six row permutations of the mixing matrix lead to the same mixing pattern. Consequently, we shall choose $P_l = 1$ without loss of generality, and thus the PMNS matrix is of the form

$$U_{\mathrm{PMNS}} = P_l U_l^\dagger \Sigma O_{3\times 3} Q_\nu$$

$$= \begin{pmatrix} \cos\theta_2 \cos\theta_3 & \cos\theta_2 \sin\theta_3 & \sin\theta_2 \\ -\cos\theta_3 \sin\theta_1 \sin\theta_2 - \cos\theta_1 \sin\theta_3 & \cos\theta_1 \cos\theta_3 - \sin\theta_1 \sin\theta_2 \sin\theta_3 & \cos\theta_2 \sin\theta_1 \\ -\cos\theta_1 \cos\theta_3 \sin\theta_2 + \sin\theta_1 \sin\theta_3 & -\cos\theta_3 \sin\theta_1 - \cos\theta_1 \sin\theta_2 \sin\theta_3 & \cos\theta_1 \cos\theta_2 \end{pmatrix} Q_\nu,$$

where the unphysical phase matrix Q_l on the far left is omitted. The mixing angles and CP-violation phases can be read off as

$$\sin^2\theta_{13} = \sin^2\theta_2, \qquad \sin^2\theta_{12} = \sin^2\theta_3, \qquad \sin^2\theta_{23} = \sin^2\theta_1,$$

$$\sin\delta_{CP} = \sin\alpha_{21} = \sin\alpha_{31} = 0. \qquad (4.19)$$

We see that all three CP phases are predicted to be trivial, and the measured values of the lepton mixing angles can be reproduced for certain values of the parameters $\theta_{1,2,3}$.

  (ii) $G_l = Z_3^T, X_\nu = S$:

    This case differs from the previous one in the value of the residual CP transformation X_ν, and we have

$$U_l = \begin{pmatrix} 1 & 0 & 0 \\ 0 & 1 & 0 \\ 0 & 0 & 1 \end{pmatrix},$$

$$\Sigma_\nu = \frac{1}{\sqrt{6}} \begin{pmatrix} 0 & 2i & \sqrt{2} \\ \sqrt{3}i & -i & \sqrt{2} \\ -\sqrt{3}i & -i & \sqrt{2} \end{pmatrix}. \qquad (4.20)$$

The six row permutations of the PMNS matrix are related through shifts in the free parameters $\theta_{1,2,3}$. We take $P_l = 1$, and then the lepton mixing angles can be extracted as follows

$$\sin^2\theta_{13} = \frac{1}{6}(3 - \cos 2\theta_1)\cos^2\theta_2,$$

$$\sin^2\theta_{12} = \sin^2\theta_3 + \frac{2(\cos 2\theta_1 + 3)\cos 2\theta_3 - 2\sin 2\theta_1 \sin \theta_2 \sin 2\theta_3}{\cos 2\theta_1 + (\cos 2\theta_1 - 3)\cos 2\theta_2 + 9},$$

$$\sin^2\theta_{23} = \frac{1}{2} - \frac{2\sqrt{3}\sin \theta_1 \sin 2\theta_2}{\cos 2\theta_1 + (\cos 2\theta_1 - 3)\cos 2\theta_2 + 9}$$

and the *CP*-odd weak basis invariants are given by

$$J_{CP} = \frac{1}{96\sqrt{6}}[-20\sin \theta_1 \sin 2\theta_3 \cos \theta_2 \cos^2\theta_1 + 4(\cos 3\theta_1 - 5\cos \theta_1)\sin 2\theta_2 \cos 2\theta_3 + (\sin 3\theta_1 - 15\sin \theta_1)\sin 2\theta_3 \cos 3\theta_2],$$

$$I_1 = \frac{(-1)^{k_1}}{36\sqrt{2}}[8\sin 2\theta_1 \sin^2\theta_2 \cos 2\theta_3 + ((7\cos 2\theta_1 + 3)\sin \theta_2 - (\cos 2\theta_1 - 3)\sin 3\theta_2)\sin 2\theta_3],$$

$$I_2 = \frac{(-1)^{k_2}}{9}[\sqrt{2}((\cos 2\theta_1 - 3)\sin \theta_2 \cos \theta_3 - \sin 2\theta_1 \sin \theta_3)\sin \theta_3 \cos^2\theta_2]. \tag{4.21}$$

We perform a numerical analysis by treating the free parameters $\theta_{1,2,3}$ as random numbers in the range of $[0, \pi]$. The three mixing angles θ_{12}, θ_{13}, and θ_{23} as well as *CP*-violating phases δ_{CP}, α_{21}, and α_{31} are calculated for each random point, and only points which agree with the global fit data at 3σ level with global fit data are retained. We plot the correlations among the mixing angles and *CP* phases in Fig. 9. We see that any value of the Dirac *CP* phase δ_{CP} in the interval $[0, 2\pi]$ can be achieved. However, the Majorana phases are strongly constrained, and their values lie in the ranges $\alpha_{21}(\text{mod } \pi) \in [0, 0.13\pi]\cup[0.87\pi, \pi]$ and $\alpha_{31}(\text{mod } \pi) \in [0, 0.25\pi]\cup[0.75\pi, \pi]$.

(iii) $G_l = Z_3^T, X_\nu = U$:

    This case is exactly the $\mu - \tau$ reflection symmetry in the charged lepton diagonal basis. One can straightforwardly read out U_l and Σ_ν as follows:

$$U_l = \begin{pmatrix} 1 & 0 & 0 \\ 0 & 1 & 0 \\ 0 & 0 & 1 \end{pmatrix}, \quad \Sigma_\nu = \frac{1}{\sqrt{2}}\begin{pmatrix} 0 & \sqrt{2}i & 0 \\ i & 0 & -1 \\ i & 0 & 1 \end{pmatrix}. \tag{4.22}$$

Out of the six possible row permutations, only $P_l = 1$ and $P_l = P_{23}$ lead to a pattern compatible with data. The PMNS matrices arising form $P_l = 1$ or $P_l = P_{23}$ are equivalent. The others give rise to either $\tan \theta_{13} = \sin \theta_{23}$ or $\tan \theta_{13} = \cos \theta_{23}$ such that the experimental data of θ_{13} and θ_{23} cannot be accommodated simultaneously. For the case of $P_l = 1$, the lepton mixing angles and the *CP*-violation phases are found to be of the form

$$\sin^2\theta_{13} = \sin^2\theta_1\cos^2\theta_2, \qquad \sin^2\theta_{23} = \frac{1}{2},$$

$$\sin^2\theta_{12} = \sin^2\theta_3 + \frac{4(\cos \theta_1 \cos 2\theta_3 - \sin \theta_1 \sin \theta_2 \sin 2\theta_3)\cos \theta_1}{\cos 2\theta_1 - 2\sin^2\theta_1 \cos 2\theta_2 + 3},$$

$$|\sin \delta_{CP}| = 1, \qquad \sin \alpha_{21} = \sin \alpha_{31} = 0. \tag{4.23}$$

Hence, both the atmospheric mixing angle θ_{23} and the Dirac phase δ_{CP} are predicted to be maximal, while the solar as well as reactor mixing angles are not constrained. There is evidence showing that the Dirac *CP*-violating phase δ_{CP} is close to $-\pi/2$ (or $3\pi/2$) [66,67]. If these data are further confirmed in the near future, this mixing pattern would be an excellent leading order approximation.

(iv) $G_l = Z_3^T, X_\nu = SU$:

    We can read out U_l and Σ_ν as

$$U_l = \begin{pmatrix} 1 & 0 & 0 \\ 0 & 1 & 0 \\ 0 & 0 & 1 \end{pmatrix},$$

$$\Sigma_\nu = \frac{1}{\sqrt{30}}\begin{pmatrix} \sqrt{6}i & 2i & -2\sqrt{5} \\ 0 & 5i & \sqrt{5} \\ 2\sqrt{6}i & -i & \sqrt{5} \end{pmatrix}. \tag{4.24}$$
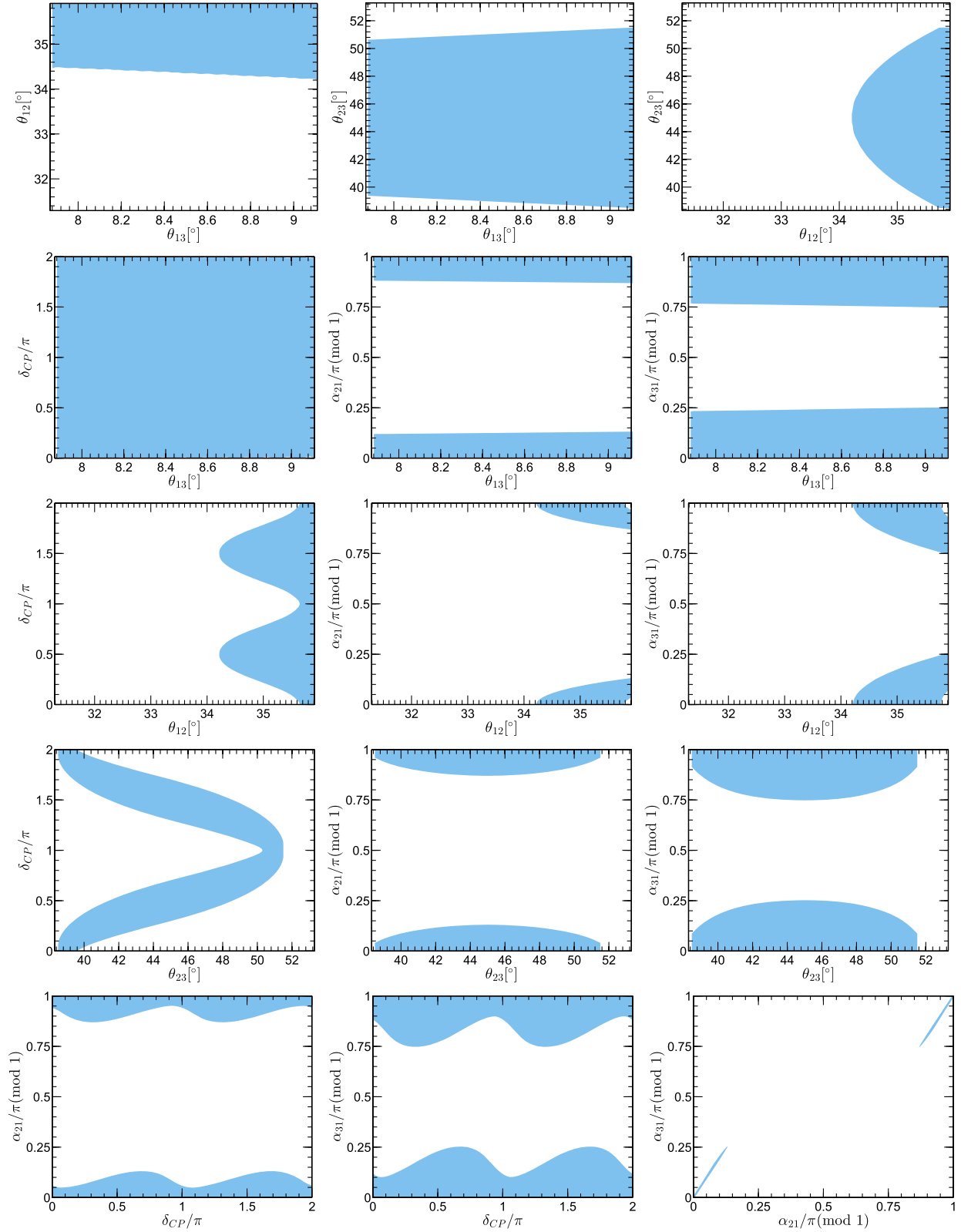
FIG. 9.   Correlations between different mixing parameters in the case of $(G_l, X_\nu) = (Z_3^T, S)$, where the three lepton mixing angles are required to be compatible with the experimental data at 3σ level [6].

For the six possible permutations of rows, only the mixing patterns with $P_l = 1$ and $P_l = P_{23}$ can accommodate the experimental data of the mixing angles for certain values of the parameters $\theta_{1,2,3}$. The PMNS matrices arising from $P_l = 1$ and $P_l = P_{23}$ are essentially the same if the redefinition of $\theta_{1,2,3}$ and relabeling of $k_{1,2}$ are taken into account. Using the actual form of the PMNS matrix given in Eq. (4.8), we find

$$\sin^2\theta_{13} = \frac{1}{15}[(\sqrt{3}\sin\theta_2 + \sqrt{2}\sin\theta_1\cos\theta_2)^2 + 10\cos^2\theta_1\cos^2\theta_2],$$

$$\sin^2\theta_{12} = \sin^2\theta_3 + \frac{4(2\cos 2\theta_1 - 3)\cos 2\theta_3 - 2(4\sin 2\theta_1\sin\theta_2 + \sqrt{6}\cos\theta_1\cos\theta_2)\sin 2\theta_3}{2\sqrt{6}\sin\theta_1\sin 2\theta_2 + 8\cos 2\theta_1\cos^2\theta_2 + 3\cos 2\theta_2 - 21},$$

$$\sin^2\theta_{23} = \frac{5(2\cos 2\theta_1 - 3)\cos^2\theta_2}{2\sqrt{6}\sin\theta_1\sin 2\theta_2 + 8\cos 2\theta_1\cos^2\theta_2 + 3\cos 2\theta_2 - 21} \qquad (4.25)$$

and

$$
\begin{aligned}
J_{CP} &= \frac{1}{144\sqrt{5}}[(\sqrt{6}\sin 3\theta_1(\cos 3\theta_2 - 5\cos\theta_2) - 2\sqrt{6}\sin\theta_1(\cos\theta_2 + 3\cos 3\theta_2) \\
&\quad + 36\sin\theta_2\cos^2\theta_2)\sin 2\theta_3 + 4\sqrt{6}(\cos 3\theta_1 - 2\cos\theta_1)\sin 2\theta_2\cos 2\theta_3], \\
I_1 &= \frac{(-1)^{k_1}}{90\sqrt{5}}[[\sqrt{6}((\cos 3\theta_2 - 5\cos\theta_2)\sin 3\theta_1 + 10\sin\theta_1\cos^3\theta_2) \\
&\quad + (25\sin\theta_2 - 7\sin 3\theta_2)\cos 2\theta_1]\sin 2\theta_3 + ((10 - 22\cos 2\theta_2)\sin 2\theta_1 + 4\sqrt{6}\sin 2\theta_2\cos 3\theta_1)\cos 2\theta_3], \\
I_2 &= \frac{(-1)^{k_2}}{90\sqrt{5}}[(5\sqrt{6}\sin\theta_1\sin\theta_2\sin 2\theta_2 - \sqrt{6}\sin 3\theta_1(\cos 3\theta_2 - 5\cos\theta_2) \\
&\quad - (5\sin\theta_2 - 7\sin 3\theta_2)\cos 2\theta_1)\sin 2\theta_3 - 10\sin 2\theta_1\cos^2\theta_2 + (17\cos 2\theta_2 + 5)\sin 2\theta_1\cos 2\theta_3 \\
&\quad - \sqrt{6}((8\cos 2\theta_1 + 1)\cos 2\theta_3 + 5)\sin 2\theta_2\cos\theta_1].
\end{aligned}
$$

The numerical results for the correlations among different mixing parameters are shown in Fig. 10. We notice that both Majorana phases α_{21} and α_{31} are determined to be around 0 and π, the solar mixing angle θ_{12} near its 3σ upper limit $\theta_{12} \sim 35°$ is preferred, and atmospheric mixing angle θ_{23} and Dirac phase δ_{CP} are correlated. The forthcoming reactor and long baseline neutrino experiments, which are expected to make precise measurement of θ_{12}, θ_{23}, and δ_{CP}, have the potential to exclude this mixing pattern.

(v) $G_l = K_4^{(S,U)}, X_\nu = T$:

The unitary transformations U_l and Σ_ν are fixed to be

$$U_l = \frac{1}{\sqrt{6}}\begin{pmatrix} 2 & \sqrt{2} & 0 \\ -1 & \sqrt{2} & \sqrt{3} \\ -1 & \sqrt{2} & -\sqrt{3} \end{pmatrix}, \qquad \Sigma_\nu = \begin{pmatrix} 1 & 0 & 0 \\ 0 & e^{-i\frac{\pi}{3}} & 0 \\ 0 & 0 & e^{i\frac{\pi}{3}} \end{pmatrix}. \qquad (4.26)$$

The agreement with experimental data on lepton mixing angles can only be achieved for $P_l = 1$, $P_l = P_{13}$, $P_l = P_{23}$, and $P_l = P_{23}P_{13}$. The two permutations $P_l = 1$ and $P_l = P_{23}$ lead to equivalent PMNS mixing matrices as $P_l = P_{13}$ and $P_l = P_{23}P_{13}$ respectively. In the case of $P_l = P_{23}P_{13}$, we can read out the mixing angles and CP invariants as follows:
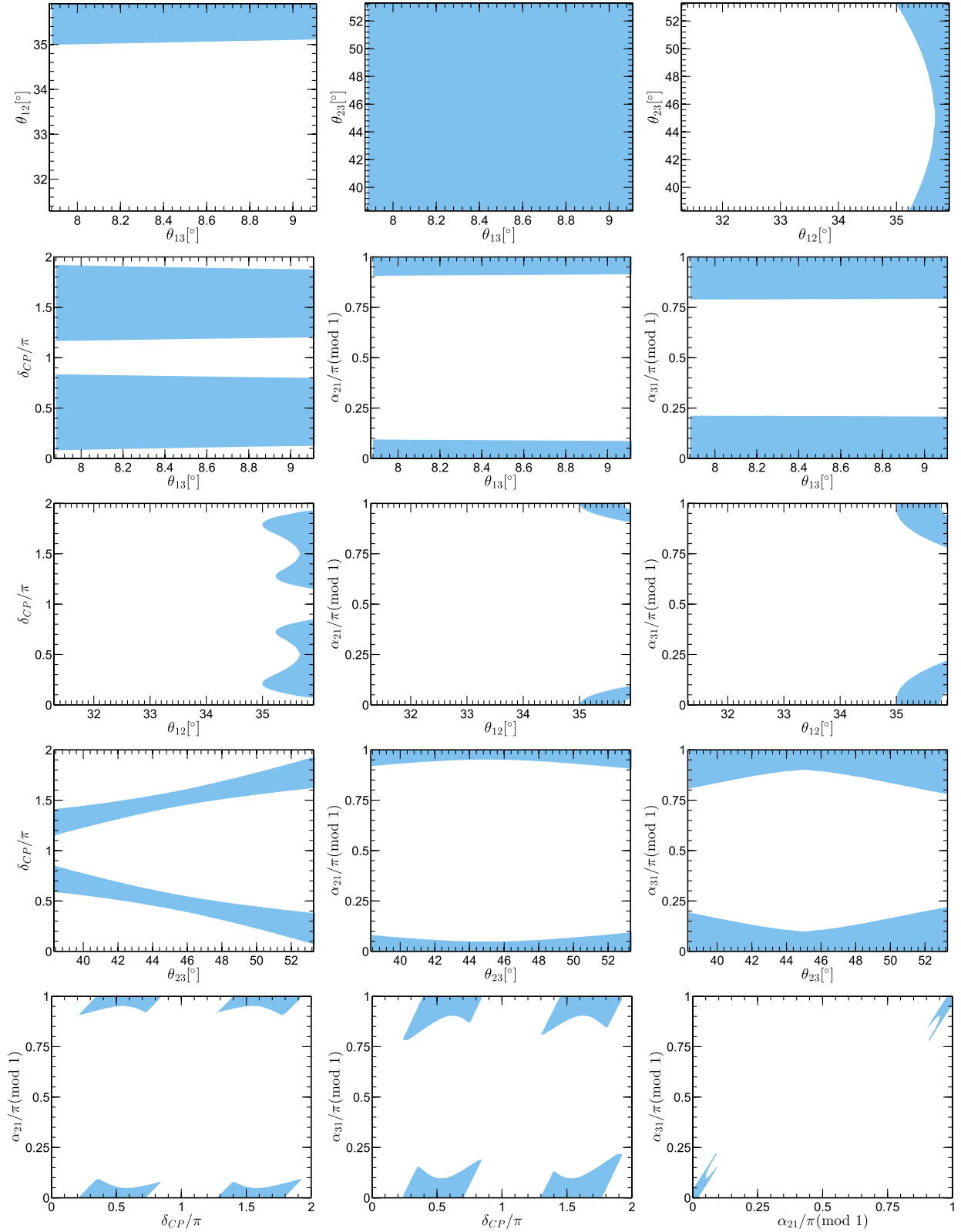
FIG. 10. Correlations between different mixing parameters in the case of $(G_l, X_\nu) = (Z_3^T, SU)$, where the three lepton mixing angles are required to be compatible with the experimental data at 3σ level [6].
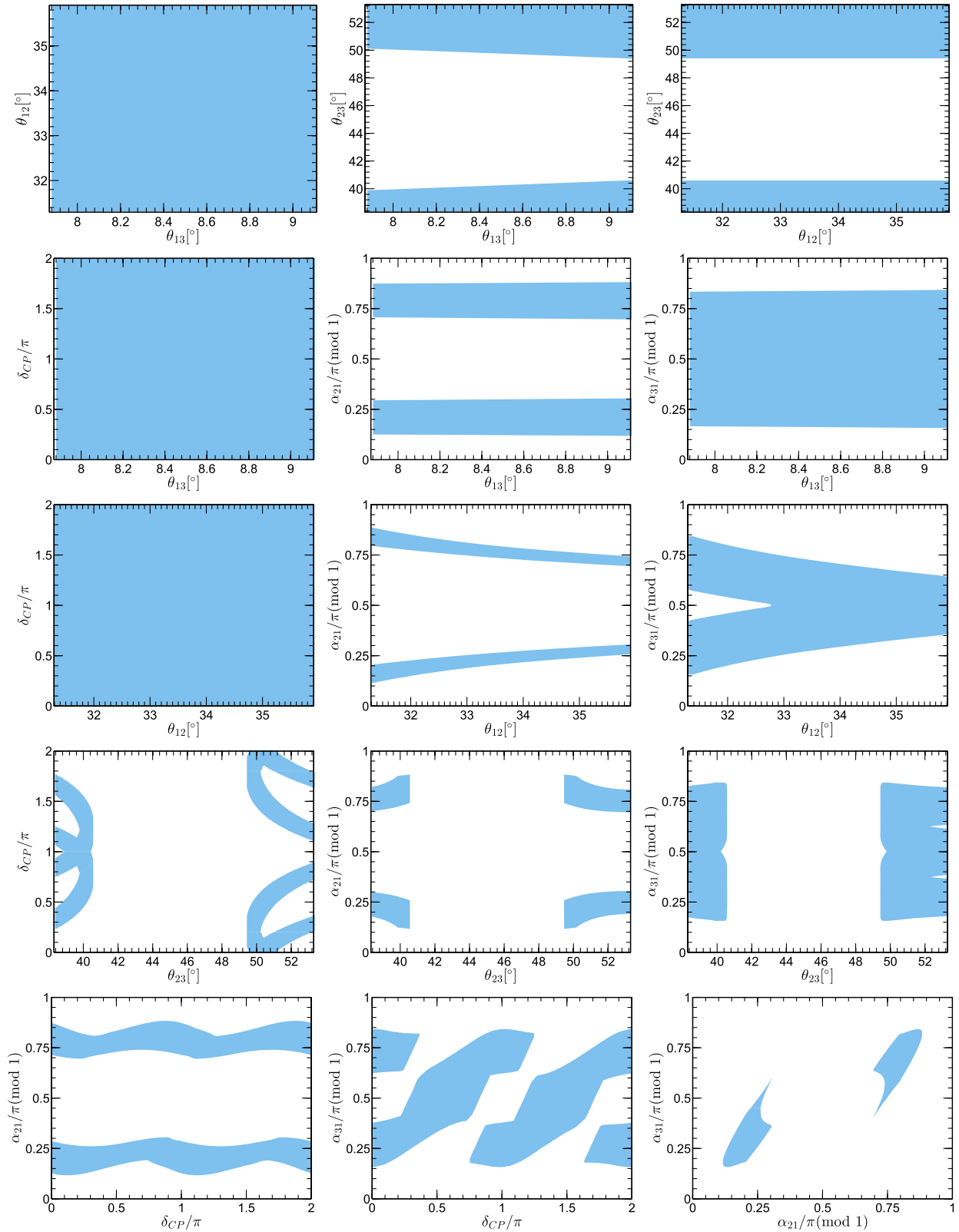
FIG. 11.　Correlations between different mixing parameters in the case of $(G_l, X_\nu) = (K_4^{(S,U)}, T)$, where the three lepton mixing angles are required to be compatible with the experimental data at 3σ level [6].
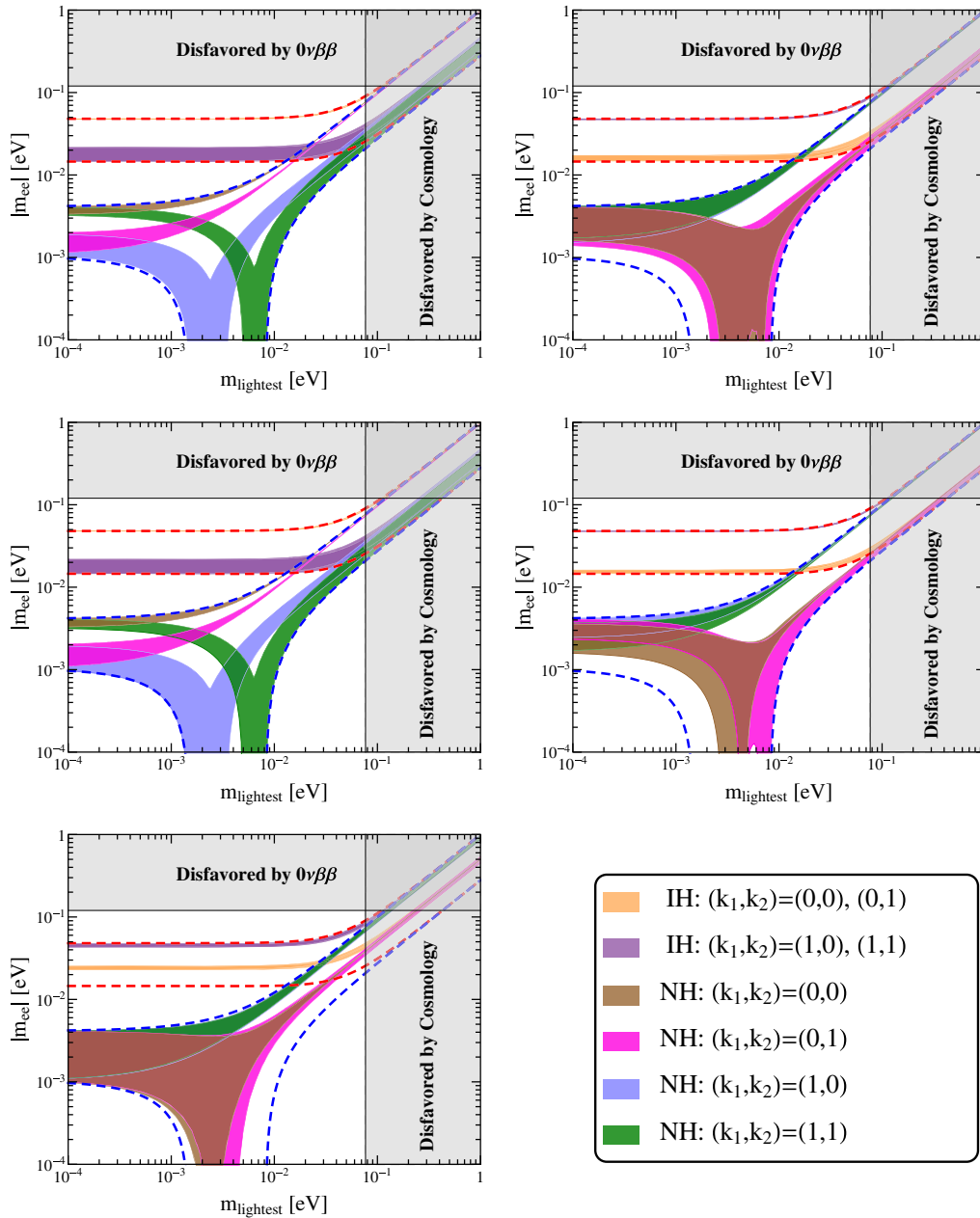
FIG. 12. The allowed regions of the effective Majorana mass $|m_{ee}|$ with respect to the lightest neutrino mass. The red (blue) dashed lines indicate the most general allowed regions for the IH (NH) neutrino mass spectrum obtained by varying the mixing parameters over their 3σ ranges [6]. The top row corresponds to the residual symmetry $(G_l, X_\nu) = (Z_3^T, 1)$ on the left and $(G_l, X_\nu) = (Z_3^T, S)$ on the right, the middle row is for $(G_l, X_\nu) = (Z_3^T, U)$ and $(G_l, X_\nu) = (Z_3^T, SU)$, and the bottom row is for $(G_l, X_\nu) = (K_4^{(S,U)}, T)$. The present most stringent upper limits $|m_{ee}| < 0.120$ eV from EXO-200 [73,74] and KamLAND-ZEN [75] are shown by the horizontal gray band. The vertical gray exclusion band is the current limit on the lightest neutrino masses from the cosmological data $\sum m_i < 0.230$ eV at 95% confidence level obtained by the Planck Collaboration [76].

$$\sin^2\theta_{13} = \frac{1}{4}(\sin 2\theta_1 + 2)\cos^2\theta_2,$$

$$\sin^2\theta_{12} = \sin^2\theta_3 + \frac{(\sin 2\theta_1 - 2)\cos 2\theta_3 + \sin\theta_2 \sin 2\theta_3 \cos 2\theta_1}{\cos 2\theta_2 + \sin 2\theta_1 \cos^2\theta_2 - 3},$$

$$\sin^2\theta_{23} = \frac{2(\sqrt{2}\sin(\theta_1 + \frac{\pi}{4})\sin 2\theta_2 - \sin^2\theta_2)}{3(\cos 2\theta_2 + \sin 2\theta_1 \cos^2\theta_2 - 3)} + \frac{1}{3},$$

$$J_{CP} = \frac{1}{128\sqrt{3}}\left[4\sin\theta_2 \sin 2\theta_3 + 4\sin 3\theta_2 \sin 2\theta_3 - 8\sqrt{2}(\sin 2\theta_1 + 2)\sin 2\theta_2 \cos\left(\theta_1 + \frac{\pi}{4}\right)\cos 2\theta_3 \right.$$

$$- 2\sqrt{2}(\sin 2\theta_1 + 4)\sin\left(\theta_1 + \frac{\pi}{4}\right)\sin 2\theta_3 \cos 3\theta_2$$

$$\left. - \sqrt{2}\left(3\sin\left(\theta_1 + \frac{\pi}{4}\right) + 5\cos\left(3\theta_1 + \frac{\pi}{4}\right)\right)\sin 2\theta_3 \cos\theta_2\right],$$

$$I_1 = \frac{(-1)^{k_1}}{32}\sqrt{3}[[(4\cos^2\theta_2 + \sin 2\theta_1(\cos 2\theta_2 - 3))\sin 2\theta_3 + 4\sin\theta_2 \cos 2\theta_1 \cos 2\theta_3]\sin\theta_2],$$

$$I_2 = \frac{(-1)^{k_2+1}}{8}\sqrt{3}[((\sin 2\theta_1 + 2)\sin\theta_2 \cos\theta_3 + \sin\theta_3 \cos 2\theta_1)\sin\theta_3 \cos^2\theta_2]. \tag{4.27}$$

For another independent permutation $P_l = P_{13}$, the atmospheric angle changes from θ_{23} to $\pi/2 - \theta_{23}$, the Dirac phase turns out to be $\pi + \delta_{CP}$, and the expressions of the other mixing parameters are not changed. The numerical results for $P_l = P_{13}$ and $P_l = P_{23}P_{13}$ are plotted in Fig. 11. There are no preferred values of δ_{CP} within the viable parameter space. The atmospheric mixing angle θ_{23} is nonmaximal, and it lies in the interval $[38.3°, 40.5°] \cup [49.5°, 51.7°]$.

Moreover, we explore the phenomenological predictions for neutrinoless double beta ($0\nu\beta\beta$) decay in each case. The effective mass $|m_{ee}|$ as a function of the lightest neutrino mass is plotted in Fig. 12. We find that $|m_{ee}|$ is around 0.015, 0.024, or 0.048 eV for the IH spectrum, while $|m_{ee}|$ depends on the neutrino masses, and it is strongly suppressed to be smaller than 10^{-4} eV for certain values of the lightest neutrino mass in the case of NH.

V. SUMMARY AND CONCLUSIONS

In recent years, discrete flavor symmetry in combination with CP symmetry has been pursued to describe the experimental data on lepton mixing in particularly to predict the CP-violating phases. Generally, it is assumed that the original flavor and CP symmetry is broken down to an Abelian subgroup and $Z_2 \times CP$ in the charged lepton and neutrino sectors respectively. In this work, we have considered other possible choices for the residual symmetry. In the first scenario, the residual subgroups preserved by the neutrino and charged lepton mass matrices are of the structure $Z_2 \times CP$. The lepton mixing matrix is found to depend on two free parameters θ_l and θ_ν, which vary between 0 and π, and generally one element is fixed to be a certain constant by the residual symmetry. The procedure to extract the PMNS mixing matrix is presented.

Moreover, we derive the criterion to determine whether two distinct remnant subgroups lead to the same mixing pattern if the freedom of redefining θ_l and θ_ν is taken into account. In order to show concrete examples and find new interesting mixing patterns, we have performed a comprehensive analysis for the popular S_4 flavor symmetry group. All possible residual groups $Z_2 \times CP$ have been considered, and we find 18 phenomenologically viable cases which can accommodate the experimentally measured values of the mixing angles for particular values of θ_l and θ_ν, as shown in Tables II–VII. This scheme is quite predictive since the allowed regions of θ_l and θ_ν are strongly constrained in order to accommodate the experimentally measured values of the mixing angles. In light of the recent experimental results of $\delta_{CP} \sim 3\pi/2$ from T2K and NOνA [66,67], the cases with $(G_l, G_\nu, X_l, X_\nu, P_l, P_\nu) = (Z_2^{ST^2SU}, Z_2^{TU}, T^2, T, P_{12}, P_{12})$, $(Z_2^{ST^2SU}, Z_2^S, T^2, SU, P_{12}, P_{13})$, $(Z_2^{ST^2SU}, Z_2^S, T^2, SU, P_{12}, P_{13})$ are preferred because they predict the Dirac phase could be 1.569π, 1.458π, and 1.542π respectively. In all 18 cases, the effective Majorana masses $|m_{ee}|$ are determined to be around 0.015, 0.028, or 0.048 eV for IH, which are within the sensitivity of the near future $0\nu\beta\beta$ decay experiments.

Discrete flavor symmetry has also been employed to explain the quark flavor mixing described by the well-known CKM matrix as well. A extensive scan of finite groups showed that only the Cabbibo mixing in the quark sector can be reproduced at leading order without resorting to special model-dependent corrections [23,78], regardless of whether the three left-handed quark fields are assigned to an irreducible triplet or doublet plus singlet. In the approach with flavor and CP symmetry, if the remnant symmetries preserved by the down and up quark mass matrices are

chosen to be an Abelian subgroup and $Z_2 \times CP$, the correct size of the quark mixing angles and CP phase still cannot be obtained. In this work, we propose the scheme with the residual symmetry $Z_2 \times CP$ in both the up and down quark sectors. The expressions for the CKM matrix and the equivalence condition are derived. From the S_4 flavor group along with a CP symmetry, we find an interesting leading order quark mixing pattern in which the experimentally preferred values of the quark mixing angles θ_{12}^q and θ_{23}^q can be accommodated, while θ_{13}^q is a bit large. It could be brought into agreement with the experimental data in a concrete model with small subleading corrections. We comment that large flavor groups can accommodate well the precisely measured CKM mixing matrix without corrections in this approach [79].

Furthermore, we consider another type of residual symmetry. The postulated flavor and CP symmetry is broken to an Abelian subgroup contained in the flavor group in the charged lepton sector and to a single remnant CP transformation in the neutrino sector. The lepton mixing angles and CP-violation phases are determined in terms of three free parameters $\theta_{1,2,3}$ in the interval $[0, \pi)$. In general, this scenario is less predictive than the previous one; each mixing parameter can vary in a relatively wide range. For an example, we find that the flavor group S_4 combined with CP symmetry gives rise to five independent mixing patterns which can describe the experimental data on lepton mixing angles. The correlation between different mixing parameters and the predictions for the neutrinoless double beta decay are studied. Given the above rich results from the S_4 group, we expect that many other new mixing patterns compatible with experimental data could be obtained in our proposal for other choices of the flavor symmetry group such as A_5 and $\Delta(6n^2)$.

In summary, among all the above phenomenologically viable cases discussed, the cases with $(G_l, G_\nu, X_l, X_\nu, P_l, P_\nu) = (Z_2^{ST^2SU}, Z_2^{TU}, T^2, T, P_{12}, P_{12})$, $(Z_2^{ST^2SU}, Z_2^S, T^2, SU, P_{12}, P_{13})$, $(Z_2^{ST^2SU}, Z_2^S, T^2, SU, P_{12}, P_{13})$ which predict $\delta_{CP} \simeq 1.569\pi$, 1.458π, and 1.542π respectively are most attractive. Their predictions for θ_{12}, θ_{23}, α_{21}, and α_{31} are distinct, as shown in Tables IV–VI, and VII. The measurement of a possible CP-violation phase in the lepton sector is very challenging and significant. The current experiments T2K and NOνA expect to be able to test the maximality of θ_{23} and δ_{CP} if running in both the neutrino and the antineutrino modes. The upcoming long baseline neutrino oscillation experiments can significantly improve the sensitivity to δ_{CP}, θ_{12}, and θ_{23}, and therefore we could exclude these mixing patterns or find strong evidence for their relevance with future facilities.

In the present work, we propose alternative schemes to understand the puzzle of quark and lepton flavor mixings from flavor and CP symmetry. The implications of our proposal for the flavor mixing are completely determined by the assumed residual symmetries and are independent of the underlying theory; they are just a consequence of group theory. It is interesting to construct explicit models to dynamically achieve the breaking patterns of flavor and CP symmetry. The required size of θ_l and θ_ν (or $\theta_{1,2,3}$) as well as the charged lepton mass hierarchy should be obtained in such models.

APPENDIX A: GROUP THEORY OF S_4

S_4 is the permutation group of four distinct objects, and geometrically it is the symmetry group of a regular octahedron. S_4 can be defined by three generators S, T, and U, which satisfy [39,42,43]

$$S^2 = T^3 = U^2 = (ST)^3 = (SU)^2 = (TU)^2 = (STU)^4 = 1. \tag{A1}$$

The 24 elements of the group belong to five conjugacy classes,

$$\begin{aligned}
1C_1 &= \{1\}, \\
3C_2 &= \{S, TST^2, T^2ST\} \\
6C_2' &= \{U, TU, SU, T^2U, STSU, ST^2SU\} \\
8C_3 &= \{T, ST, TS, STS, T^2, ST^2, T^2S, ST^2S\} \\
6C_4 &= \{STU, TSU, T^2SU, ST^2U, TST^2U, T^2STU\},
\end{aligned} \tag{A2}$$

where kC_n designates a conjugacy class of k elements of which the order is n. The group structure of S_4 has been studied in detail in Ref. [80]. The residual flavor symmetry group can only be in the Abelian group in order to avoid the degenerate mass spectrum. The Abelian subgroups of S_4 are given as follows:
  (i) Z_2 subgroups:

$$\begin{aligned}
Z_2^{ST^2SU} &= \{1, ST^2SU\}, & Z_2^{TU} &= \{1, TU\}, \\
Z_2^{STSU} &= \{1, STSU\}, & Z_2^{T^2U} &= \{1, T^2U\}, \\
Z_2^U &= \{1, U\}, & Z_2^{SU} &= \{1, SU\}, \\
Z_2^S &= \{1, S\}, & Z_2^{T^2ST} &= \{1, T^2ST\}, \\
Z_2^{TST^2} &= \{1, TST^2\}, & & \tag{A3}
\end{aligned}$$

where the superscripts denote the generators of the subgroups. The first six Z_2 subgroups are related to each other by group conjugation, and the last three subgroups are conjugate to each other as well.

(ii) Z_3 subgroups:

$$Z_3^{ST} = \{1, ST, T^2S\}, \qquad Z_3^T = \{1, T, T^2\},$$
$$Z_3^{STS} = \{1, STS, ST^2S\}, \qquad Z_3^{TS} = \{1, TS, ST^2\}.$$
$$\text{(A4)}$$

All the above Z_3 subgroups are conjugate among each other.

(iii) Z_4 subgroups:

$$Z_4^{TST^2U} = \{1, TST^2U, S, T^2STU\},$$
$$Z_4^{ST^2U} = \{1, ST^2U, TST^2, T^2SU\},$$
$$Z_4^{TSU} = \{1, TSU, T^2ST, STU\}, \qquad \text{(A5)}$$

which are related with each other under group conjugation.

(iv) K_4 subgroups:

$$K_4^{(S,TST^2)} \equiv Z_2^S \times Z_2^{TST^2} = \{1, S, TST^2, T^2ST\},$$
$$K_4^{(S,U)} \equiv Z_2^S \times Z_2^U = \{1, S, U, SU\},$$
$$K_4^{(TST^2,T^2U)} \equiv Z_2^{TST^2} \times Z_2^{T^2U}$$
$$\equiv \{1, TST^2, T^2U, ST^2SU\},$$
$$K_4^{(T^2ST,TU)} \equiv Z_2^{T^2ST} \times Z_2^{TU}$$
$$= \{1, T^2ST, TU, STSU\}, \qquad \text{(A6)}$$

where $K_4^{(S,TST^2)}$ is a normal subgroup of S_4 and the remaining three K_4 subgroups are conjugate to each other.

The group S_4 has five irreducible representations: two singlets **1** and **1'**, one doublet **2**, and two triplets **3** and **3'**. The representation matrices for the generators S, T, and U in each of the irreducible representations are summarized in Table VIII. Notice that the representations **3** and **3'** differ in the overall sign of the generator U. As has been shown in previous work [39,42], the generalized CP transformation compatible with the S_4 flavor symmetry is of the same form as the flavor group transformation in our working basis.

TABLE VIII. The representation matrices of the generators S, T, and U in different irreducible representations of S_4, where $\omega = e^{2\pi i/3}$.

	S	T	U
1, 1'	1	1	± 1
2	$\begin{pmatrix} 1 & 0 \\ 0 & 1 \end{pmatrix}$	$\begin{pmatrix} \omega & 0 \\ 0 & \omega^2 \end{pmatrix}$	$\begin{pmatrix} 0 & 1 \\ 1 & 0 \end{pmatrix}$
3, 3'	$\frac{1}{3}\begin{pmatrix} -1 & 2 & 2 \\ 2 & -1 & 2 \\ 2 & 2 & -1 \end{pmatrix}$	$\begin{pmatrix} 1 & 0 & 0 \\ 0 & \omega^2 & 0 \\ 0 & 0 & \omega \end{pmatrix}$	$\mp\begin{pmatrix} 1 & 0 & 0 \\ 0 & 0 & 1 \\ 0 & 1 & 0 \end{pmatrix}$

APPENDIX B: EQUIVALENCE CONDITIONS FOR TWO CKM MATRICES WITH $|a_1| = |b_1| \neq 0, 1$

Following the methods in Secs. II B and III, we can find out the criterion to determine whether two distinct residual symmetries of the structure $Z_2 \times CP$ in both the up and down type quark sectors lead to the same CKM matrix for the general case with $|a_1| = |b_1| \neq 0, 1$, if possible shifts of the free parameters θ_u and θ_d are considered. The expression for the combination $U_q \equiv \Sigma_u^\dagger \Sigma_d$ is written as Eq. (3.8). One can always set a_1 and b_1 to be real and positive by redefining the quark fields. We shall report the results in the following:

(i) $b_2^2 + b_3^2 \neq 0$, $b_4^2 + b_7^2 \neq 0$:

In this case, the conditions under which essentially the same quark mixing is obtained are given by

$$|a_2^2 + a_3^2| = |b_2^2 + b_3^2|,$$
$$(a_2b_2 + a_3b_3)(a_2^*b_3^* - a_3^*b_2^*) \in \mathbb{R},$$
$$|a_4^2 + a_7^2| = |b_4^2 + b_7^2|,$$
$$(a_4b_4 + a_7b_7)(a_4^*b_7^* - a_7^*b_4^*) \in \mathbb{R},$$
$$a_5 = \frac{(xb_5 + yb_6)z + (xb_8 + yb_9)w}{(b_2^2 + b_3^2)(b_4^2 + b_7^2)},$$
$$a_6 = \frac{(xb_6 - yb_5)z + (xb_9 - yb_8)w}{(b_2^2 + b_3^2)(b_4^2 + b_7^2)},$$
$$a_8 = \frac{(xb_8 + yb_9)z - (xb_5 + yb_6)w}{(b_2^2 + a_3^2)(b_4^2 + b_7^2)},$$
$$a_9 = \frac{(xb_9 - yb_8)z - (xb_6 - yb_5)w}{(b_2^2 + b_3^2)(b_4^2 + b_7^2)}, \qquad \text{(B1)}$$

with

$$x \equiv a_2b_2 + a_3b_3, \qquad y \equiv a_2b_3 - a_3b_2,$$
$$z \equiv a_4b_4 + a_7b_7, \qquad w \equiv a_4b_7 - a_7b_4. \qquad \text{(B2)}$$

(ii) $b_2^2 + b_3^2 = 0$, $b_4^2 + b_7^2 \neq 0$:

The equivalent conditions are found to be

$$a_2b_2 + a_3b_3 = 0,$$
$$|a_4^2 + a_7^2| = |b_4^2 + b_7^2|,$$
$$(a_4b_4 + a_7b_7)(a_4^*b_7^* - a_7^*b_4^*) \in \mathbb{R},$$
$$t_iT_j - t_jT_i = 0,$$
$$t_i/T_i \in \mathbb{R},$$
$$\text{with} \quad i, j = 5, 6, 8, 9, \qquad \text{(B3)}$$

where

$$t_5 = va_5b_2 - (zb_5 + wb_8)a_2, \qquad t_6 = -va_6b_2 + (zb_6 + wb_9)a_2,$$
$$t_8 = va_8b_2 - (zb_8 - wb_5)a_2, \qquad t_9 = -va_9b_2 + (zb_9 - wb_6)a_2,$$
$$T_5 = -iva_5b_2 - i(zb_6 + wb_9)a_3, \qquad T_6 = iva_6b_2 - i(zb_5 + wb_8)a_3,$$
$$T_8 = -iva_8b_2 - i(zb_9 - wb_6)a_3, \qquad T_9 = iva_9b_2 - i(zb_8 - wb_5)a_3, \tag{B4}$$

with

$$v \equiv b_4^2 + b_7^2. \tag{B5}$$

(iii) $b_2^2 + b_3^2 \neq 0$, $b_4^2 + b_7^2 = 0$:

The resulting CKM matrices would be related through redefinition of the parameters θ_u and θ_d if the following constraints are fulfilled,

$$a_4b_4 + a_7b_7 = 0, \qquad |a_2^2 + a_3^2| = |b_2^2 + b_3^2|, \qquad (a_2b_2 + a_3b_3)(a_2^*b_3^* - a_3^*b_2^*) \in \mathbb{R},$$
$$t_i'T_j' - t_j'T_i' = 0, \qquad t_i'/T_i' \in \mathbb{R}, \quad \text{with} \quad i, j = 5, 6, 8, 9, \tag{B6}$$

where

$$t_5' = ua_5b_4 - (xb_5 + yb_6)a_4, \qquad t_6' = ua_6b_4 - (xb_6 - yb_5)a_4,$$
$$t_8' = -ua_8b_4 + (xb_8 + yb_9)a_4, \qquad t_9' = -ua_9b_4 + (xb_9 - yb_8)a_4,$$
$$T_5' = -iua_5b_4 - i(xb_8 + yb_9)a_7, \qquad T_6' = -iua_6b_4 - i(xb_9 - yb_8)a_7,$$
$$T_8' = iua_8b_4 - i(xb_5 + yb_6)a_7, \qquad T_9' = iua_9b_4 - i(xb_6 - yb_5)a_7, \tag{B7}$$

with

$$u \equiv b_2^2 + b_3^2. \tag{B8}$$

(iv) $b_2^2 + b_3^2 = 0$, $b_4^2 + b_7^2 = 0$:

The postulated residual symmetries would give rise to the same quark mixing pattern if the following conditions are satisfied:

$$a_2b_2 + a_3b_3 = 0, \qquad a_4b_4 + a_7b_7 = 0, \qquad a_2^2a_4(b_2b_5 - b_3b_6) = b_2^2b_4(a_2a_5 - a_3a_6). \tag{B9}$$

Note that the above results are valid up to the transformations in Eq. (3.18).

[1] T. Kajita, Rev. Mod. Phys. **88**, 030501 (2016).

[2] A. B. McDonald, Rev. Mod. Phys. **88**, 030502 (2016).

[3] Special Issue on Neutrino oscillations: Celebrating the Nobel Prize in Physics 2015, edited by T. Ohlsson, Nucl. Phys. **B908**, 1 (2016).

[4] F. Capozzi, G. L. Fogli, E. Lisi, A. Marrone, D. Montanino, and A. Palazzo, Phys. Rev. D **89**, 093018 (2014).

[5] D. V. Forero, M. Tortola, and J. W. F. Valle, Phys. Rev. D **90**, 093006 (2014).

[6] M. C. Gonzalez-Garcia, M. Maltoni, and T. Schwetz, J. High Energy Phys. 11 (2014) 052.

[7] F. Capozzi, E. Lisi, A. Marrone, D. Montanino, and A. Palazzo, Nucl. Phys. **B908**, 218 (2016).

[8] K. Abe et al. (T2K Collaboration), Phys. Rev. D **91**, 072010 (2015).

[9] G. Altarelli and F. Feruglio, Rev. Mod. Phys. **82**, 2701 (2010).

[10] H. Ishimori, T. Kobayashi, H. Ohki, Y. Shimizu, H. Okada, and M. Tanimoto, Prog. Theor. Phys. Suppl. **183**, 1 (2010).

[11] S. F. King and C. Luhn, Rep. Prog. Phys. **76**, 056201 (2013).

[12] S. F. King, A. Merle, S. Morisi, Y. Shimizu, and M. Tanimoto, New J. Phys. **16**, 045018 (2014).

[13] S. F. King, J. Phys. G **42**, 123001 (2015).

[14] K. Abe et al. (T2K Collaboration), Phys. Rev. Lett. **107**, 041801 (2011).

[15] P. Adamson *et al.* (MINOS Collaboration), Phys. Rev. Lett. **107**, 181802 (2011).

[16] Y. Abe *et al.* (Double Chooz Collaboration), Phys. Rev. Lett. **108**, 131801 (2012); Phys. Rev. D **86**, 052008 (2012).

[17] F. P. An *et al.* (Daya Bay Collaboration), Phys. Rev. Lett. **108**, 171803 (2012); Chin. Phys. C **37**, 011001 (2013).

[18] J. K. Ahn *et al.* (RENO Collaboration), Phys. Rev. Lett. **108**, 191802 (2012).

[19] M. Holthausen, K. S. Lim, and M. Lindner, Phys. Lett. B **721**, 61 (2013).

[20] S. F. King, T. Neder, and A. J. Stuart, Phys. Lett. B **726**, 312 (2013).

[21] R. M. Fonseca and W. Grimus, J. High Energy Phys. 09 (2014) 033.

[22] J. Talbert, J. High Energy Phys. 12 (2014) 058.

[23] C. Y. Yao and G. J. Ding, Phys. Rev. D **92**, 096010 (2015).

[24] F. Feruglio, C. Hagedorn, and R. Ziegler, J. High Energy Phys. 07 (2013) 027.

[25] P. Chen, G. J. Ding, F. Gonzalez-Canales, and J. W. F. Valle, Phys. Lett. B **753**, 644 (2016).

[26] P. Chen, G. J. Ding, F. Gonzalez-Canales, and J. W. F. Valle, Phys. Rev. D **94**, 033002 (2016).

[27] P. Chen, C. C. Li, and G. J. Ding, Phys. Rev. D **91**, 033003 (2015).

[28] L. L. Everett, T. Garon, and A. J. Stuart, J. High Energy Phys. 04 (2015) 069.

[29] P. Chen, C. Y. Yao, and G. J. Ding, Phys. Rev. D **92**, 073002.

[30] W. Grimus and M. N. Rebelo, Phys. Rep. **281**, 239 (1997).

[31] M. Holthausen, M. Lindner, and M. A. Schmidt, J. High Energy Phys. 04 (2013) 122.

[32] M. C. Chen, M. Fallbacher, K. T. Mahanthappa, M. Ratz, and A. Trautner, Nucl. Phys. **B883**, 267 (2014).

[33] G. J. Ding, S. F. King, and A. J. Stuart, J. High Energy Phys. 12 (2013) 006.

[34] C. C. Nishi, Phys. Rev. D **93**, 093009 (2016).

[35] G. N. Li and X. G. He, Phys. Lett. B **750**, 620 (2015).

[36] E. Ma, Phys. Rev. D **92**, 051301 (2015).

[37] C. C. Li, J. N. Lu, and G. J. Ding, Nucl. Phys. **B913**, 110 (2016).

[38] R. N. Mohapatra and C. C. Nishi, Phys. Rev. D **86**, 073007 (2012).

[39] G. J. Ding, S. F. King, C. Luhn, and A. J. Stuart, J. High Energy Phys. 05 (2013) 084.

[40] F. Feruglio, C. Hagedorn, and R. Ziegler, Eur. Phys. J. C **74**, 2753 (2014).

[41] C. Luhn, Nucl. Phys. **B875**, 80 (2013).

[42] C. C. Li and G. J. Ding, Nucl. Phys. **B881**, 206 (2014).

[43] C. C. Li and G. J. Ding, J. High Energy Phys. 08 (2015) 017.

[44] C. C. Li and G. J. Ding, J. High Energy Phys. 05 (2015) 100.

[45] A. Di Iura, C. Hagedorn, and D. Meloni, J. High Energy Phys. 08 (2015) 037.

[46] P. Ballett, S. Pascoli, and J. Turner, Phys. Rev. D **92**, 093008 (2015).

[47] J. Turner, Phys. Rev. D **92**, 116007 (2015).

[48] G. C. Branco, I. de Medeiros Varzielas, and S. F. King, Phys. Rev. D **92**, 036007 (2015).

[49] G. C. Branco, I. de Medeiros Varzielas, and S. F. King, Nucl. Phys. **B899**, 14 (2015).

[50] G. J. Ding and Y. L. Zhou, Chin. Phys. C **39**, 021001 (2015).

[51] G. J. Ding and Y. L. Zhou, J. High Energy Phys. 06 (2014) 023.

[52] G. J. Ding and S. F. King, Phys. Rev. D **89**, 093020 (2014).

[53] S. j. Rong, arXiv:1604.08482.

[54] C. Hagedorn, A. Meroni, and E. Molinaro, Nucl. Phys. **B891**, 499 (2015).

[55] G. J. Ding and S. F. King, Phys. Rev. D **93**, 025013 (2016).

[56] S. F. King and T. Neder, Phys. Lett. B **736**, 308 (2014).

[57] G. J. Ding, S. F. King, and T. Neder, J. High Energy Phys. 12 (2014) 007.

[58] C. C. Li, C. Y. Yao, and G. J. Ding, J. High Energy Phys. 05 (2016) 007.

[59] C. Y. Yao and G. J. Ding, Phys. Rev. D **94**, 073006 (2016).

[60] C. Hagedorn and E. Molinaro, arXiv:1602.04206.

[61] P. Chen, G. J. Ding, and S. F. King, J. High Energy Phys. 03 (2016) 206.

[62] I. Girardi, S. T. Petcov, A. J. Stuart, and A. V. Titov, Nucl. Phys. **B902**, 1 (2016); I. Girardi, S. T. Petcov, and A. V. Titov, Nucl. Phys. **B911**, 754 (2016).

[63] C. Jarlskog, Phys. Rev. Lett. **55**, 1039 (1985).

[64] G. C. Branco, L. Lavoura, and M. N. Rebelo, Phys. Lett. B **180**, 264 (1986); E. E. Jenkins and A. V. Manohar, Nucl. Phys. **B792**, 187 (2008); G. C. Branco, R. G. Felipe, and F. R. Joaquim, Rev. Mod. Phys. **84**, 515 (2012).

[65] K. A. Olive *et al.* (Particle Data Group Collaboration), Chin. Phys. C **38**, 090001 (2014).

[66] K. Iwamoto (for the T2K Collaboration), ICHEP 2016, Chicago, 2016 (unpublished), http://indico.cern.ch/event/432527/contributions/2143636/.

[67] J. Bian (for the NOνA Collaboration), ICHEP 2016, Chicago, 2016 (unpublished), http://indico.cern.ch/event/432527/contributions/2144798/.

[68] F. An *et al.* (JUNO Collaboration), J. Phys. G **43**, 030401 (2016).

[69] S. B. Kim, Nucl. Part. Phys. Proc. **265–266**, 93 (2015).

[70] R. Acciarri *et al.* (DUNE Collaboration), arXiv:1601.05471; R. Acciarri *et al.* (DUNE Collaboration), arXiv:1512.06148; J. Strait *et al.* (DUNE Collaboration), arXiv:1601.05823; R. Acciarri *et al.* (DUNE Collaboration), arXiv:1601.02984.

[71] E. Kearns *et al.* (Hyper-Kamiokande Working Group Collaboration), arXiv:1309.0184.

[72] K. Abe *et al.* (Hyper-Kamiokande Working Group Collaboration), arXiv:1412.4673.

[73] M. Auger *et al.* (EXO-200 Collaboration), Phys. Rev. Lett. **109**, 032505 (2012).

[74] J. B. Albert *et al.* (EXO-200 Collaboration), Nature (London) **510**, 229 (2014).

[75] A. Gando *et al.* (KamLAND-Zen Collaboration), Phys. Rev. Lett. **110**, 062502 (2013).

[76] P. A. R. Ade *et al.* (Planck Collaboration), Astron. Astrophys. **571**, A16 (2014).

[77] M. Bona *et al.* (UTfit Collaboration), J. High Energy Phys. 10 (2006) 081; for updated results of the global fit, see http://www.utfit.org/UTfit/.

[78] M. Holthausen and K. S. Lim, Phys. Rev. D **88**, 033018 (2013).

[79] C. C. Li and G. J. Ding (unpublished).

[80] G. J. Ding, Nucl. Phys. **B827**, 82 (2010).